

Forecasting range shifts of a dioecious plant species under climate change

Jacob K. Moutouama 0000-0003-1599-1671^{*1}, Aldo Compagnoni 0000-0001-8302-7492², and Tom E.X. Miller 0000-0003-3208-6067¹

¹Program in Ecology and Evolutionary Biology, Department of BioSciences, Rice University, Houston, TX USA

²Institute

of Biology, Martin Luther University Halle-Wittenberg, Halle, Germany; and German Centre for Integrative Biodiversity Research (iDiv), Leipzig, Germany

Running header: Forecasting range shifts

Keywords: demography, forecasting, global warming, matrix projection model, population dynamics, sex ratio, range limits

Submitted to: *Ecology letters* (Letter)

Data accessibility statement: All data used in this paper are publicly available and cited appropriately (Miller and Compagnoni, 2022a). Should the paper be accepted, all computer scripts supporting the results will be archived in a Zenodo package, with the DOI included at the end of the article. During peer review, our code (Stan, Bash and R) is available at <https://github.com/jmoutouama/POAR-Forecasting>.

Conflict of interest statement: None.

Authorship statement: J.K.M., A.C. and T.E.X.M. designed the study. A.C. and T.E.X.M. collected the data. All authors conducted the statistical analyses and modeling. J.K.M. drafted the manuscript, and T.E.X.M contributed to revisions.

Abstract:

Main Text:

Figures: 6

Tables: 0

References: 106

*Corresponding author: jmoutouama@gmail.com

¹ Abstract

² Global climate change has triggered an urgent need for predicting the reorganization of Earth's
³ biodiversity. Currently, the vast majority of models used to forecast population viability and
⁴ range shifts in response to climate change ignore the complication of sex structure, and thus
⁵ the potential for females and males to differ in their sensitivity to climate drivers. We developed
⁶ demographic models of range limitation, parameterized from geographically distributed com-
⁷ mon garden experiments, with females and males of a dioecious grass species (*Poa arachnifera*)
⁸ throughout and beyond its range in the south-central U.S. Female-dominant and two-sex
⁹ model versions both predict that future climate change will alter population viability and
¹⁰ will induce a poleward niche shift beyond current northern limits. However, the magnitude of
¹¹ niche shift was underestimated by the female-dominant model, because females have broader
¹² temperature tolerance than males and become mate-limited under female-biased sex ratios.
¹³ Our result illustrate how explicit accounting for both sexes could enhance population viability
¹⁴ forecasts and conservation planning for dioecious species in response to climate change.

15 **Introduction**

16 Rising temperatures and extreme drought events associated with global climate change are
17 leading to increased concern about how species will become redistributed across the globe
18 under future climate conditions (Bertrand et al., 2011; Gamelon et al., 2017; Smith et al., 2024).
19 Species' range limits, when not driven by dispersal limitation, should generally reflect the limits
20 of the ecological niche (Lee-Yaw et al., 2016). Niches and geographic ranges are often limited
21 by climatic factors including temperature and precipitation (Sexton et al., 2009). Therefore,
22 any substantial changes in the magnitude of these climatic factors could impact population
23 viability, with implications for range expansions or contractions based on which regions of
24 a species' range become more or less suitable (Davis and Shaw, 2001; Pease et al., 1989).

25 Forecasting range shifts for dioecious species (most animals and ca. 7% of plant species)
26 is complicated by the potential for sexual niche differentiation, i.e. distinct responses of
27 females and males to shared climate drivers (Hultine et al., 2016; Morrison et al., 2016; Pottier
28 et al., 2021; Tognetti, 2012). The lower cost of reproduction for one sex (male or female)
29 may allow that sex to invest its energy in other functions that produce higher growth rates,
30 greater clonality, or even higher survival rates compared to the other sex, leading to sexual
31 niche differentiation (Bruijning et al., 2017). Accounting for sexual niche differentiation
32 is a long-standing challenge in accurately predicting which sex will successfully track
33 environmental change and how this will impact population viability and range shifts (Gissi
34 et al., 2023; Jones et al., 1999). Populations in which males are rare under current climatic
35 conditions could experience low reproductive success due to sperm or pollen limitation that
36 may lead to population decline in response to climate change that disproportionately favors
37 females (Eberhart-Phillips et al., 2017). In contrast, climate change could expand male habitat
38 suitability (e.g. upslope movement), which might increase seed set for mate-limited females
39 and favor range expansion (Petry et al., 2016). Across dioecious plants, for example, studies
40 suggest that future climate change toward hotter and drier conditions may favor male-biased
41 sex ratios (Field et al., 2013; Hultine et al., 2016). Although the response of species to climate
42 warming is an urgent and active area of research, few studies have disentangled the interaction
43 between sex and climate drivers to understand their combined effects on population dynamics
44 and range shifts, despite calls for such an approach (Gissi et al., 2023; Hultine et al., 2016).

45 The vast majority of theory and models in population biology, including those used
46 to forecast biodiversity responses to climate change, ignore the complication of sex structure
47 (but see Ellis et al., 2017; Gissi et al., 2024; Pottier et al., 2021). Traditional approaches instead
48 focus exclusively on females, assuming that males are in sufficient supply as to never limit
49 female fertility. In contrast, "two-sex" models are required to fully account for demographic

50 differences between females and males and sex-specific responses to shared climate drivers
51 (Gerber and White, 2014; Miller et al., 2011). Sex differences in maturation, reproduction,
52 and mortality schedules can generate skew in the operational sex ratio (OSR; sex ratio of
53 individuals available for mating) even if the birth sex ratio is 1:1 (Eberhart-Phillips et al., 2017;
54 Shelton, 2010). Climate and other environmental drivers can therefore influence the OSR
55 via their influence on sex-specific demographic rates. In a two-sex framework, demographic
56 rates both influence and respond to the OSR in a feedback loop that makes two-sex models
57 inherently nonlinear and more data-hungry than corresponding female-dominant models.
58 Given the additional complexity and data needs, forecasts of range dynamics for dioecious
59 species under future climate change that explicitly account for females, males, and their
60 inter-dependence are limited (Lynch et al., 2014; Petry et al., 2016).

61 Tracking the impact of climate change on population viability (λ) and distributional
62 limits of dioecious taxa depends on our ability to build mechanistic models that take into
63 account the spatial and temporal context of sex specific response to climate change, while
64 accounting for sources of uncertainty (Davis and Shaw, 2001; Evans et al., 2016). Structured
65 population models built from demographic data collected from geographically distributed
66 observations or common garden experiments provide several advantages for studying
67 the impact of climate change on species' range shifts (Merow et al., 2017; Schultz et al.,
68 2022; Schwinning et al., 2022). First, demographic models link individual-level life history
69 events (mortality, development, and regeneration) to population demography, allowing the
70 investigation of factors explaining vital rate responses to environmental drivers (Dahlgren
71 et al., 2016; Ehrlén and Morris, 2015; Louthan et al., 2022). Second, demographic models
72 have a natural interface with statistical estimation of individual-level vital rates that provide
73 quantitative measures of uncertainty and isolate different sources of variation, features that
74 can be propagated to population-level predictions (Elderd and Miller, 2016; Ellner et al.,
75 2022). Finally, structured demographic models can be used to identify which aspects of
76 climate are the most important drivers of population dynamics. For example, Life Table
77 Response Experiments (LTRE) built from structured models have become widely used to
78 understand the relative importance of covariates in explaining variation in population growth
79 rate (Czachura and Miller, 2020; Ellner et al., 2016; Hernández et al., 2023).

80 In this study, we combined geographically-distributed common garden experiments,
81 hierarchical Bayesian statistical modeling, two-sex population projection modeling, and climate
82 back-casting and forecasting to understand demographic responses to climate change and their
83 implications for past, present, and future range dynamics. Our work focused on the dioecious
84 plant Texas bluegrass (*Poa arachnifera*), which is distributed along environmental gradients
85 in the south-central U.S. corresponding to variation in temperature across latitude and

86 precipitation across longitude (Fig. 1A)¹. This region has experienced rapid climate warming
87 since 1900 and this is projected to continue through the end of the century (Fig. 1 B and C). Our
88 previous study showed that, despite evidence for differentiation of climatic niche between sexes,
89 the female niche mattered the most in driving longitudinal range limits of Texas bluegrass
90 (Miller and Compagnoni, 2022b). However, that study used a single proxy variable (longitude)
91 to represent environmental variation related to aridity and did not consider variation in
92 temperature, which is the much stronger dimension of forecasted climate change in this region
93 (Fig. S-2). Developing a rigorous forecast for the implications of future climate change requires
94 that we transition from implicit to explicit treatment of multiple climate drivers, as we do
95 here. Leveraging the power of Bayesian inference, we take a probabilistic view of past, present,
96 and future range limits by quantifying the probability of population viability ($Pr(\lambda \geq 1)$) in
97 relation to climate drivers of demography, an approach that fully accounts for uncertainty
98 arising from multiple sources of estimation and process error. Specifically, we asked:

- 99 1. What are the sex-specific vital rate responses to variation in temperature and precipitation
100 across the species' range?
- 101 2. How do sex-specific vital rates combine to determine the influence of climate variation
102 on population growth rate (λ)?
- 103 3. What is the impact of climate change on operational sex ratio throughout the range?
- 104 4. What are the likely historical and projected dynamics of the Texas bluegrass geographic
105 niche and how does accounting for sex structure modify these predictions?

106 Materials and methods

107 Study species and climate context

108 Texas bluegrass (*Poa arachnifera*) is a dioecious perennial, summer-dormant cool-season (C3)
109 grass that occurs in the south-central U.S. (Texas, Oklahoma, and southern Kansas) (Figure
110 1) (Hitchcock, 1971). Texas bluegrass grows between October and May, flowers in spring,
111 and goes dormant during the hot summer months of June to September (Kindiger, 2004).
112 Following this life history, we divided the calendar year into growing (October 1 - May
113 31) and dormant (June 1 - September 30) seasons in the analyses below. Biological sex is
114 genetically based and the birth (seed) sex ratio is 1:1 (Renganayaki et al., 2005). Females and
115 males are morphologically indistinguishable except for their inflorescences. Like all grasses,
116 this species is wind pollinated (Hitchcock, 1971) and most male-female pollen transfer occurs

¹Fig. A does not show what we are saying here. Maybe I should add the Figure with the raster

¹¹⁷ within 10-15m (Compagnoni et al., 2017). Surveys of 22 natural populations throughout the
¹¹⁸ species' distribution indicated that operational sex ratio (the female fraction of inflorescences)
¹¹⁹ ranged from 0.007 to 0.986 with a mean of 0.404 (Miller and Compagnoni, 2022b).

¹²⁰ Latitudinal limits of the Texas bluegrass distribution span 7.74 °C to 16.94 °C of
¹²¹ temperature during the dormant season and 24.38 °C to 28.80 °C during the dormant season.
¹²² Longitudinal limits span 244.9 mm to 901.5 mm of precipitation during the growing season
¹²³ and 156.3 mm to 373.3 mm. This region has experienced *ca.* 0.5 °C of climate warming since
¹²⁴ 1900, with faster warming during the cool-season months ($0.0055^{\circ}\text{C}/\text{yr}$) than the hot summers
¹²⁵ ($0.0046^{\circ}\text{C}/\text{yr}$) (Fig. S-1). Future warming is projected to accelerate to $0.03 - 0.06^{\circ}\text{C}/\text{yr}$ by
¹²⁶ the end of the century depending on the season and forecast model. On the other hand,
¹²⁷ precipitation has increased over the past century for much of the region but is forecasted
¹²⁸ to decline back to early-20th century levels (Fig. S-1). ²

¹²⁹ Common garden experiment

¹³⁰ Experimental design

¹³¹ We conducted a range-wide common garden experiment to quantify sex-specific demographic
¹³² responses to climate variation. Details of the experimental design are provided in Miller
¹³³ and Compagnoni (2022b); we provide a brief overview here. The experiment was installed
¹³⁴ at 14 sites throughout and, in some cases, beyond the natural range of Texas bluegrass that
¹³⁵ sampled a broad range of latitude and longitude (Figure 1A). At each site, we established
¹³⁶ 14 blocks. For each block we planted three female and three male individuals that were
¹³⁷ clonally propagated from females and males from eight natural source populations (Figure
¹³⁸ 1A); because sex is genetically-based, clones never deviated from their expected sex. The
¹³⁹ experiment was established in November 2013 with a total of 588 female and 588 male plants,
¹⁴⁰ and was censused in May of 2014, 2015, and 2016. At each census, we collected data on
¹⁴¹ survival, size (number of tillers), and number of panicles (reproductive inflorescences). For
¹⁴² the analyses that follow, we focus on the 2014-15 and 2015-16 transition years, since the start
¹⁴³ of the experiment did not include the full 2013-14 transition year.

²*I like this but I don't know if this not a repetition of what we've said in the introduction about climate change in the study area.*

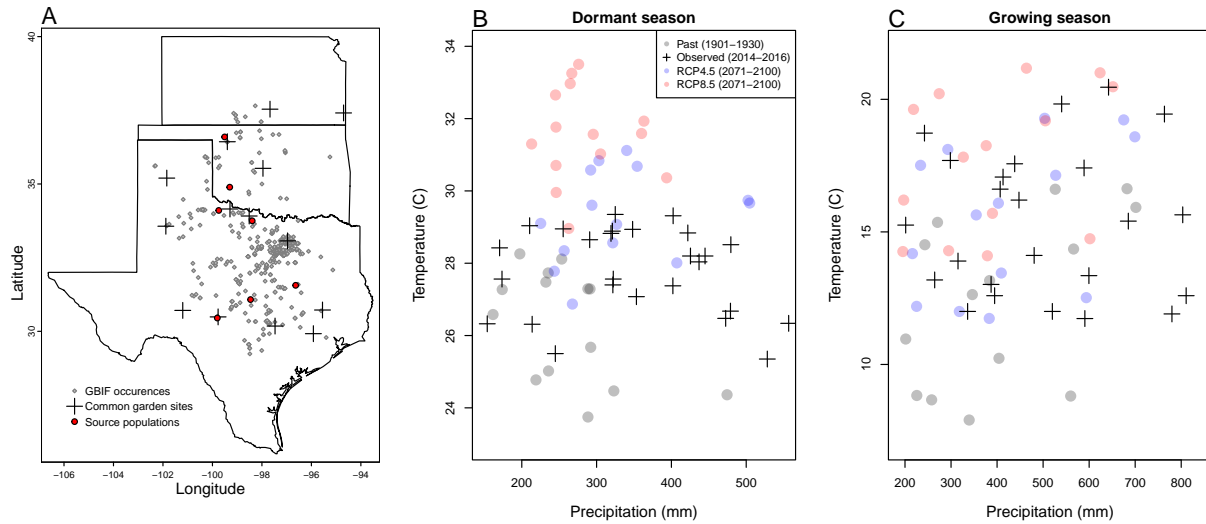


Figure 1: Experimental gardens and climate of the study region. **A:** Map of 14 experimental garden sites (crosses) in Texas, Oklahoma, and Kansas relative to GBIF occurrences of *Poa arachnifera* (gray points). Red points indicate source populations for plants used in the common garden experiment. **B,C:** Past, future, and observed climate space for growing and dormant seasons. Crosses show observed conditions for the sites and years of the common garden experiment. Gray points show historical (1901-1930) climate normals, and blue and red points show end-of-century (2071-2100) climate normals for RCP4.5 and RCP8.5 projections, respectively, from MIROC5. See also (Figure ?? for more information about historical and projected climate change in the study region.

144 Climatic data collection

145 We gathered downscaled monthly temperature and precipitation for each site from Chelsa
 146 (Karger et al., 2017) to describe observed climate conditions during our study period. These
 147 climate data were used as covariates in vital rate regressions. We aligned the climatic years
 148 to match demographic transition years (June 1 – May 31) and growing and dormant seasons
 149 within each year. To back-cast and forecast demographic responses to changes in climate
 150 throughout the study region, we also gathered projection data for three 30-year periods: “past”
 151 (1901-1930), “current” (1990-2019) and “future” (2070-2100). Data for future climatic periods
 152 were downloaded from four general circulation models (GCMs) selected from the Coupled
 153 Model Intercomparison Project Phase 5 (CMIP5): Model for Interdisciplinary Research on
 154 Climate (MIROC5), Australian Community Climate and Earth System Simulator (ACCESS1-3),
 155 Community Earth System Model (CESM1-BGC), Centro Euro-Mediterraneo sui Cambiamenti
 156 Climatici Climate Model (CMCC-CM). All the GCMs were also downloaded from Chelsa
 157 (Sanderson et al., 2015). We evaluated future climate projections from two scenarios of
 158 representative concentration pathways (RCPs): RCP4.5, an intermediate-to-pessimistic scenario
 159 assuming a radiative forcing amounting to 4.5 W m^{-2} by 2100, and RCP8.5, a pessimistic

¹⁶⁰ emission scenario which projects a radiative forcing of 8.5 Wm^{-2} by 2100 (Schwalm et al.,
¹⁶¹ 2020; Thomson et al., 2011).

¹⁶² Projection data for the three 30-year periods included warmer or colder conditions than ob-
¹⁶³ served in our experiment, so extending our inferences to these conditions required some extrap-
¹⁶⁴ olation. However, across all sites, both study years were 1-2°C warmer than their correspond-
¹⁶⁵ ing “current” (1990-2019) temperature normals (Fig. S-2). Additionally, the 2014–15 growing
¹⁶⁶ season was generally wetter and cooler across the study region than 2015–16 (Fig. S-2). Com-
¹⁶⁷ bined, the geographic and inter-annual replication of the common garden experiment provided
¹⁶⁸ good coverage of most past and future conditions throughout the study region (Fig. 1B,C).

¹⁶⁹ **Sex-specific demographic responses to climatic variation across common garden sites**

¹⁷⁰ We used individual-level measurements of survival, growth (change in number of tillers), flow-
¹⁷¹ ering, and number of panicles (conditional on flowering) to develop Bayesian mixed effect mod-
¹⁷² els describing how each vital rate varies as a function of sex, size, and four climate covariates
¹⁷³ (precipitation and temperature of growing and dormant season)(Supplementary Method S.2.1).
¹⁷⁴ These vital rate models included main effects of size (the natural log of tiller number), sex, and
¹⁷⁵ seasonal climate covariates. Climate variables were fit with second-degree polynomial func-
¹⁷⁶ tions to accommodate the possibility of hump-shaped relationships (reduced demographic per-
¹⁷⁷ formance at both extremes). We also included two-way interactions between sex and each cli-
¹⁷⁸ mate driver and between temperature and precipitation within each season, and a three-way in-
¹⁷⁹ teraction between sex, temperature, and precipitation within each season. We modeled survival
¹⁸⁰ and flowering data with a Bernoulli distribution and the growth (tiller number) with a zero-
¹⁸¹ truncated Poisson inverse Gaussian distribution. Fertility (panicle count conditional on flower-
¹⁸² ing) was modeled as zero-truncated negative binomial. We used generic, weakly informative
¹⁸³ priors to fit coefficients for survival, growth, flowering models ($\beta \sim N(0, 1.5)$) and random
¹⁸⁴ effect variances ($\sigma \sim \text{Gamma}(\gamma(0.1, 0.1))$). We fit fertility model with also weakly informative pri-
¹⁸⁵ ors for coefficients ($\beta \sim N(0, 0.15)$). Different priors were used for fertility because the panicle
¹⁸⁶ model has a large number of parameters relative to the amount of available data (subset of our
¹⁸⁷ data) and because these specifics priors help prevent the model from overfitting. Each vital rate
¹⁸⁸ also includes normally distributed random effects for block-to-block variation ($\phi \sim N(0, \sigma_{block})$),
¹⁸⁹ site to site variation ($\nu \sim N(0, \sigma_{site})$), and source-to-source variation that is related to the genetic
¹⁹⁰ provenance of the transplants used to establish the common garden ($\rho \sim N(0, \sigma_{source})$).

191 **Sex ratio responses to climatic variation across common garden sites**

192 We also used the experimental data to investigate how climatic variation across the range
193 influenced sex ratio and operational sex ratio of the common garden populations. To do so,
194 we developed two Bayesian linear models using data collected during three years. Each model
195 had OSR or SR as response variable and a climate variable (temperature and precipitation
196 of the growing season and dormant season) as predictor (Supplementary Method S.2.2). We
197 modeled the OSR or SR data with a Bernoulli distribution and used non informative priors
198 for each coefficient ($\omega \sim N(0, 100)$).

200 **Model-fitting procedures**

201 All models were fit using Stan (Stan Development Team, 2023) in R 4.3.1 (R Core Team,
202 2023). We centered and standardized all climatic predictors to mean zero, variance one, which
203 facilitated model convergence. We ran three chains for 1000 samples for warmup and 4000
204 for sampling, with a thinning rate of 3. We assessed the quality of the models using posterior
predictive checks (Piironen and Vehtari, 2017) (Figure S-3).

205 **Two-sex and female-dominant matrix projection models**

206 We used the climate-dependent vital rate regressions estimated above, combined with
207 additional data sources, to build female-dominant and two-sex versions of a climate-explicit
208 matrix projection model (MPMs) structured by the discrete state variables size (number
209 of tillers) and sex. The female-dominant and two-sex versions of the model both allow
210 for sex-specific response to climate and differ only in the feedback between operational
211 sex ratio and seed fertilization. For clarity of presentation we do not explicitly include
212 climate-dependence in the notation below, but the following model was evaluated over
213 variation in seasonal temperature and precipitation.

214 Let $F_{x,t}$ and $M_{x,t}$ be the number of female and male plants of size x in year t , where
215 $x \in [1, \dots, U]$. The minimum possible size is one tiller and U is the 95th percentile of observed
216 maximum size (35 tillers). Let F_t^R and M_t^R be new female and male recruits in year t , which
217 we treat as distinct from the rest of the size distribution because we assume they do not
218 reproduce in their first year, consistent with our observations. For a pre-breeding census,
219 the expected numbers of recruits in year $t+1$ is given by:

$$220 F_{t+1}^R = \sum_1^U [p^F(x) \cdot c^F(x) \cdot d \cdot v(\mathbf{F}_t, \mathbf{M}_t) \cdot m \cdot \rho] F_{x,t} \quad (1)$$

221

$$M_{t+1}^R = \sum_1^U [p^F(x) \cdot c^F(x) \cdot d \cdot v(\mathbf{F}_t, \mathbf{M}_t) \cdot m \cdot (1 - \rho)] F_{x,t} \quad (2)$$

222 where p^F and c^F are flowering probability and panicle production for females of size x , d
 223 is the number of seeds per female panicle, v is the probability that a seed is fertilized, m is
 224 the probability that a fertilized seed germinates, and ρ is the primary sex ratio (proportion
 225 of recruits that are female), which we assume to be 0.5 (Miller and Compagnoni, 2022b).

226 In the two-sex model, seed fertilization is a function of population structure, allowing for
 227 feedback between vital rates and operational sex ratio (OSR). In the context of the model, OSR
 228 is defined as the fraction of panicles that are female and is derived from the $U \times 1$ vectors
 229 \mathbf{F}_t and \mathbf{M}_t :

230

$$v(\mathbf{F}_t, \mathbf{M}_t) = v_0 * \left[1 - \left(\frac{\sum_1^U p^F(x, z) c^F(x, z) F_{x,t}}{\sum_1^U p^F(x, z) c^F(x, z) F_{x,t} + p^M(x, z) c^M(x, z) M_{x,t}} \right)^\alpha \right] \quad (3)$$

231 The summations tally the total number of female and male panicles over the size distribution,
 232 giving the fraction of total panicles that are female. We focus on the female fraction of
 233 panicles and not female fraction of reproductive individuals because panicle number can vary
 234 widely depending on size; we assume that few males with many panicles vs. many males
 235 with few panicles are interchangeable pollination environments. Eq. 3 has the properties
 236 that seed fertilization is maximized at v_0 as OSR approaches 100% male, goes to zero as OSR
 237 approaches 100% female, and parameter α controls how female seed viability declines as male
 238 panicles become rare. We estimated these parameters using data from a sex ratio manipulation
 239 experiment, conducted in the center of the range, in which seed fertilization was measured
 240 in plots of varying OSR; this experiment is described elsewhere (Compagnoni et al., 2017) and
 241 is summarized in [Supplementary Method S.2.3](#)³. This experiment also provided estimates for
 242 seed number per panicle (d) and germination rate (m). Lacking data on climate-dependence,
 243 we assume that seed fertilization, seed number, and germination rate do not vary with climate.

244 The dynamics of the size-structured component of the population are given by:

245

$$F_{y,t+1} = [\sigma \cdot g^F(y, x=1)] F_t^R + \sum_L^U [s^F(x) \cdot g^F(y, x)] F_{x,t} \quad (4)$$

246

$$M_{y,t+1} = [\sigma \cdot g^M(y, x=1)] M_t^R + \sum_L^U [s^M(x) \cdot g^M(y, x)] M_{x,t} \quad (5)$$

247 The first terms indicate recruits that survived their first year and enter the size distribution
 248 of established plants. We estimated the seedling survival probability σ using demographic

³I think the supplement should also include a data figure showing the fit of the model to the experimental data.

249 data from the congeneric species *Poa autumnalis* in east Texas (T.E.X. Miller and J.A. Rudgers,
250 *unpublished data*), and we assume that σ is the same across sexes and climatic variables. We did
251 this because we had little information on the early life cycle transitions of greenhouse-raised
252 transplants. We used $g(y, x=1)$ (the future size distribution of one-tiller plants from the
253 transplant experiment) to give the probability that a surviving recruit reaches size y . The
254 second component of the equations indicates survival and size transition of established
255 plants from the previous year, where s and g give the probabilities of surviving at size x and
256 growing from sizes x to y , respectively, and superscripts indicate that these functions may
257 be unique to females (F) and males (M).

258 The model described above yields a $2(U+1) \times 2(U+1)$ transition matrix. We estimated
259 the population growth rate λ of the female dominant model as the leading eigenvalue of
260 the transition matrix. Since the two-sex MPM is nonlinear (matrix elements affect and are
261 affected by population structure) we estimated λ and stable sex ratio (female fraction of all
262 individuals) and operational sex ratio (female fraction of panicles) by numerical simulation.
263 Since all parameters were estimated using MCMC sampling, we were able to propagate the
264 uncertainty in our estimates of the vital rate parameters to uncertainty in λ . Furthermore,
265 by sampling over distributions associated with site, block, and source population variance
266 terms, we are able to incorporate process error into the total uncertainty in λ , in addition
267 to the uncertainty that arises from imperfect knowledge of the parameter values. For example,
268 sampling over site and block variances accounts for regional and local spatial heterogeneity
269 that is not explained by climate, and sampling over source population variance accounts for
270 genetically-based demographic differences across the species' range.

271 Life Table Response Experiments

272 We conducted two types of Life Table Response Experiments (LTRE) to isolate contributions of
273 climate variables and sex-specific vital rates to variation in λ . First, to identify which aspect of
274 climate is most important for population viability, we used an LTRE based on a nonparametric
275 model for the dependence of λ on parameters associated with seasonal temperature and
276 precipitation (Ellner et al., 2016). To do so, we used the RandomForest package to fit a
277 regression model with four climatic variables (temperature of growing season, precipitation of
278 growing season, temperature of the dormant season and precipitation of the dormant season)
279 as predictors and λ calculated from the two sex model as response (Liaw et al., 2002). The
280 regression model allowed the estimation of the relative importance of each predictor.

281 Second, to understand how climate drivers influence λ via sex-specific demography, we
282 decomposed the effect of each climate variable on population growth rate (λ) into contribution

283 arising from the effect on each female and male vital rate using a “regression design” LTRE
284 (Caswell, 1989, 2000). This LTRE decomposes the sensitivity of λ to climate according to:

285

$$\frac{\partial \lambda}{\partial \text{climate}} \approx \sum_i \frac{\partial \lambda}{\partial \theta_i^F} \frac{\partial \theta_i^F}{\partial \text{climate}} + \frac{\partial \lambda}{\partial \theta_i^M} \frac{\partial \theta_i^M}{\partial \text{climate}} \quad (6)$$

286 where, θ_i^F and θ_i^M represent sex-specific parameters (the regression coefficients of the vital
287 rate functions). Because LTRE contributions are additive, we summed across vital rates to
288 compare the total contributions of female and male parameters.⁴⁵

289 Population viability across the climatic niche and geographic range

290 To understand how climate shapes the niche and geographic range of Texas bluegrass, we
291 estimated the probability of self-sustaining populations ($\Pr(\lambda \geq 1)$) conditional to temperature
292 and precipitation of the dormant and growing seasons. $\Pr(\lambda > 1)$ was calculated for the
293 two-sex model and the female dominant MPMs using the proportion of the 300 posterior
294 samples that lead to a $\lambda \geq 1$ (Diez et al., 2014). Population viability in climate niche space
295 was then represented as a contour plot with values of $\Pr(\lambda > 1)$ at given temperature and
296 precipitation for the growing season, holding dormant season climate constant, and vice versa.

297 $\Pr(\lambda > 1)$ was also mapped onto geographic layers of three US states (Texas, Oklahoma
298 and Kansas) to delineate past, current and future potential geographic distribution of the
299 species. To do so, we estimated $\Pr(\lambda > 1)$ conditional to all climate covariates for each
300 pixel ($\sim 25 \text{ km}^2$) for each time period (past, present, future). Because of the amount of the
301 computation involved, we use 100 posterior samples to estimate $\Pr(\lambda > 1)$ across the study
302 area (Texas, Oklahoma and Kansas).

303 Results

304 Sex specific demographic response and sex ratio variation across climatic 305 conditions

306 We found strong demographic responses to climate drivers across our Texas bluegrass
307 common garden sites and years, and evidence for demographic differences between the sexes.
308 Regression coefficients related to sex and/or sex:size interactions were significantly non-zero

⁴Let's talk about this

⁵I do not agree. It is true that you can compute this, but only by “turning off” the interaction by holding the interacting variable constant. I still think this needs to be better addressed in both LTRE analyses.

309 (95% credible intervals excluding zero) for most vital rates (Fig. S-4), suggesting sexual
310 divergence in demography. Females generally had an advantage over males, especially in
311 survival and flowering (Fig. 2). **That female demographic advantage was more pronounce for**
312 **extreme values of climate (Fig. S-5, Fig. S-6).**⁶ Vital rate regressions also revealed significant
313 interactions between sex and climate drivers, especially in vegetative growth (Fig. S-4)B.⁷

⁶*I added the 3D plots for vital rates to show that female individuals do better in extreme climate*

⁷*I am skipping the rest of this section for now because I think we need a different visualization for the vital rates. I also think this section should include the common garden sex ratio results, since they are connected to the vital rate responses.*

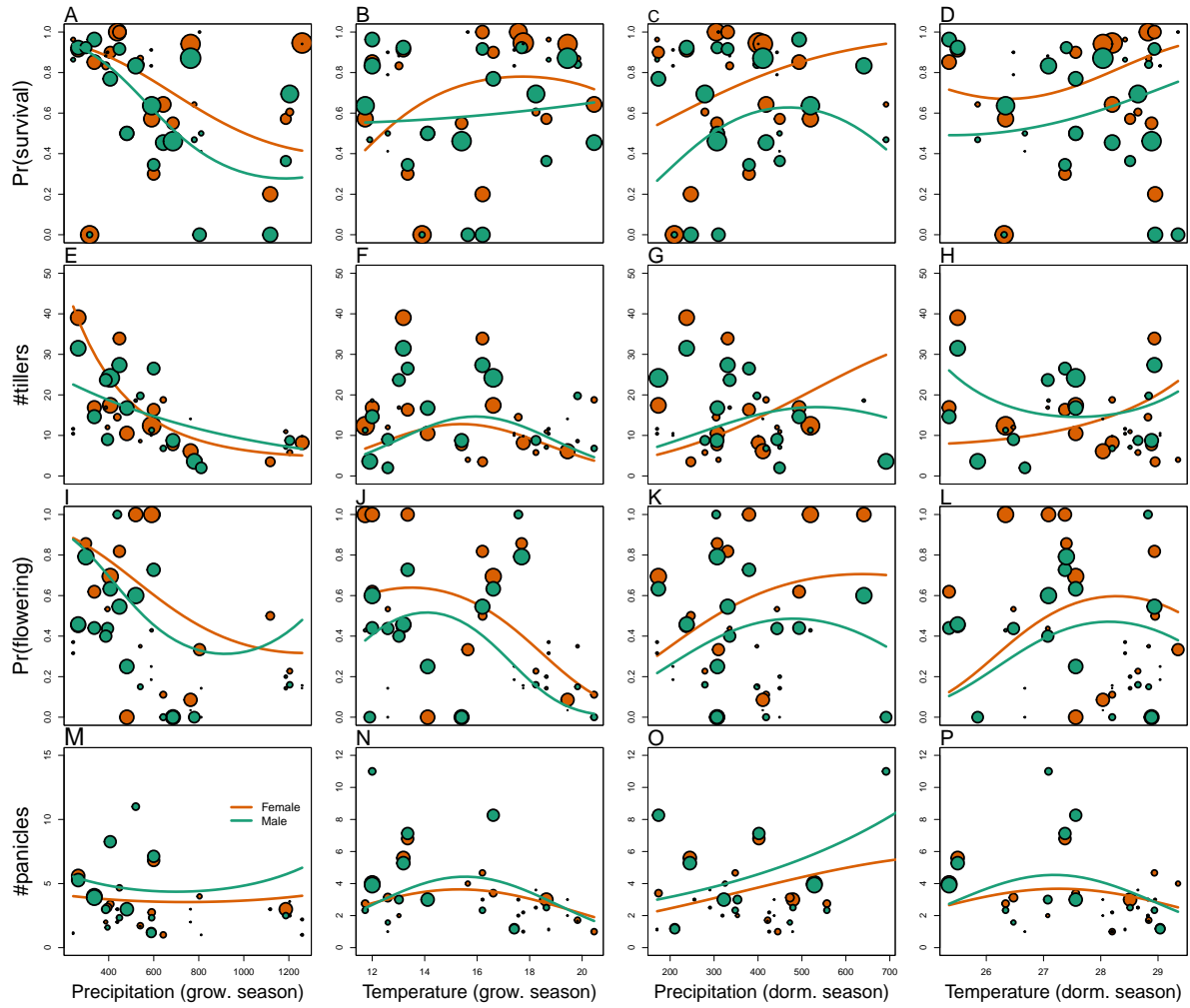


Figure 2: Sex specific demographic response to climate across species range. (A, B, C, D) Probability of survival as a function of precipitation and temperature of the growing and dormant season. (E, F, G, H) Change in number of tillers as a function of precipitation and temperature of the growing and dormant season. (I, J, K, L) Probability of flowering as a function of precipitation and temperature of growing and dormant season. (M, N, O, P) Change in number of panicles as a function of precipitation and temperature of the growing and dormant season. Points show means by site for females (orange) and males (green). Points sizes are proportional to the sample sizes of the mean and are jittered. Lines show fitted statistical models for females (orange) and males (green) based on posterior mean parameter values. Lower panels below each data panel show the posterior distribution of the difference between females and males as a function of climate (positive and negative values indicate female and male advantage, respectively); dashed horizontal line shows zero difference.

314 Across common garden sites, operational sex ratio (proportion of female panicles) of the
 315 experimental populations was female-biased on average (STATS), reflecting the overall greater
 316 rates of female vs. male flowering rather than bias in the underlying population composition
 317 (all sites were planted with equal numbers of females and males). Across sites and years, OSR
 318 variation was significantly predicted by [describe sex ratio analyses].⁸

⁸I am not sure what the new sex ratio results look like, so not sure if we are keeping this.

319 **Climate drivers of population viability across niche space**

320 Putting all vital rates together in the MPM framework reveals how climate shapes fitness
321 variation across niche dimensions and geographic space, and how accounting for sex structure
322 modifies these inferences. Figure 3 shows the estimated probability of population viability
323 ($\lambda \geq 1$) across seasonal climate niche space; these probabilities account for uncertainty in the
324 vital rate parameters as well as process error related to spatial heterogeneity and genotypic
325 variation. For both female-dominant and two-sex models, fitness variation across niche space
326 was dominated by temperature, with weaker effects of precipitation (compare vertical and
327 horizontal contours in Fig. 3). These visual trends are supported by LTRE decomposition
328 indicating that variation in fitness across climatic conditions is most strongly driven by
329 responses to growing and dormant season temperature, with weaker interactive effects of
330 precipitation that modulate the effects of temperature (Figure S-11). LTRE analysis also showed
331 that declines in population viability at high and low temperatures were driven most strongly
332 by reductions in vegetative growth and panicle production, with stronger contributions from
333 females than males (Figure S-12).⁹ Intermediate temperatures of both growing and dormant
334 seasons were associated with near-certain projections of population viability ($Pr(\lambda \geq 1) \approx 1$),
335 and high and low temperature extremes during both seasons were associated with low niche
336 suitability ($Pr(\lambda \geq 1) < 0.2$). Higher precipitation slightly expanded the range of suitable
337 temperatures during the dormant season (Fig. 3A), and the reverse was true in the growing
338 season (Fig. 3B). Points in Fig. 3 show that climate change forecasted for the common
339 garden locations would move many of them toward lower-suitability regions of niche space
340 associated with high growing and dormant season temperatures (see also Fig. S-13).¹⁰

341 While the female-dominant and two-sex models were generally in agreement about
342 high confidence in intermediate temperature optima, they differed around the edges of niche
343 space (Fig. 3C,D¹¹,S-13). The female-dominant model over-predicted population viability,
344 especially with respect to growing season temperature. For example, the female-dominant
345 model predicted¹² that, for most levels of precipitation, warm average growing season (winter)
346 temperatures of $\sim 20^{\circ}\text{C}$ had high suitability ($Pr(\lambda \geq 1) > 0.9$), while the two-sex model
347 indicated that these conditions were most likely unsuitable ($Pr(\lambda \geq 1) < 0.5$). Similarly, at
348 low winter temperatures that the two-sex model identifies with high certainty as unsuitable
349 ($Pr(\lambda \geq 1) < 0.1$), the female-dominant model is more optimistic ($Pr(\lambda \geq 1) > 0.4$). Across

⁹You can see here that I am suggesting we moved the lambda vs climate figure to an appendix. If you disagree we can keep it, but I think the niche space results are the better figure to show.

¹⁰I think we should redraw this without contours so that the points are more readable. I would also change the point types and sizes.

¹¹All multi-panel figures need letter labels.

¹²I think I am switching tenses. We will need to clean this up.

³⁵⁰ growing season climate space, the female-dominant model over-estimates population viability
³⁵¹ by ca. 10%, on average (Fig. 3D, Fig. S-14B). The difference between female-dominant and
³⁵² two-sex models was qualitatively similar but weaker in magnitude for niche dimensions of
³⁵³ the dormant season (Fig. 3C, Fig. S-14A).

³⁵⁴ Female-dominant and two-sex models diverged most strongly in regions of niche
³⁵⁵ space that favored strongly female-biased operational sex ratios (Fig. WE NEED A FIGURE
³⁵⁶ FOR THIS). This suggests mate limitation as the biological mechanism underlying model
³⁵⁷ differences. The two-sex model accounts for feedbacks between OSR and female fertility, with
³⁵⁸ reduced seed viability at OSR exceeding ~ 75% female panicles (Fig. WE NEED A FIGURE
³⁵⁹ FOR THIS). Lacking this feedback, the female-dominant model over-predicts population
³⁶⁰ viability in regions of niche space where male flowering is not sufficient to maximize seed set.

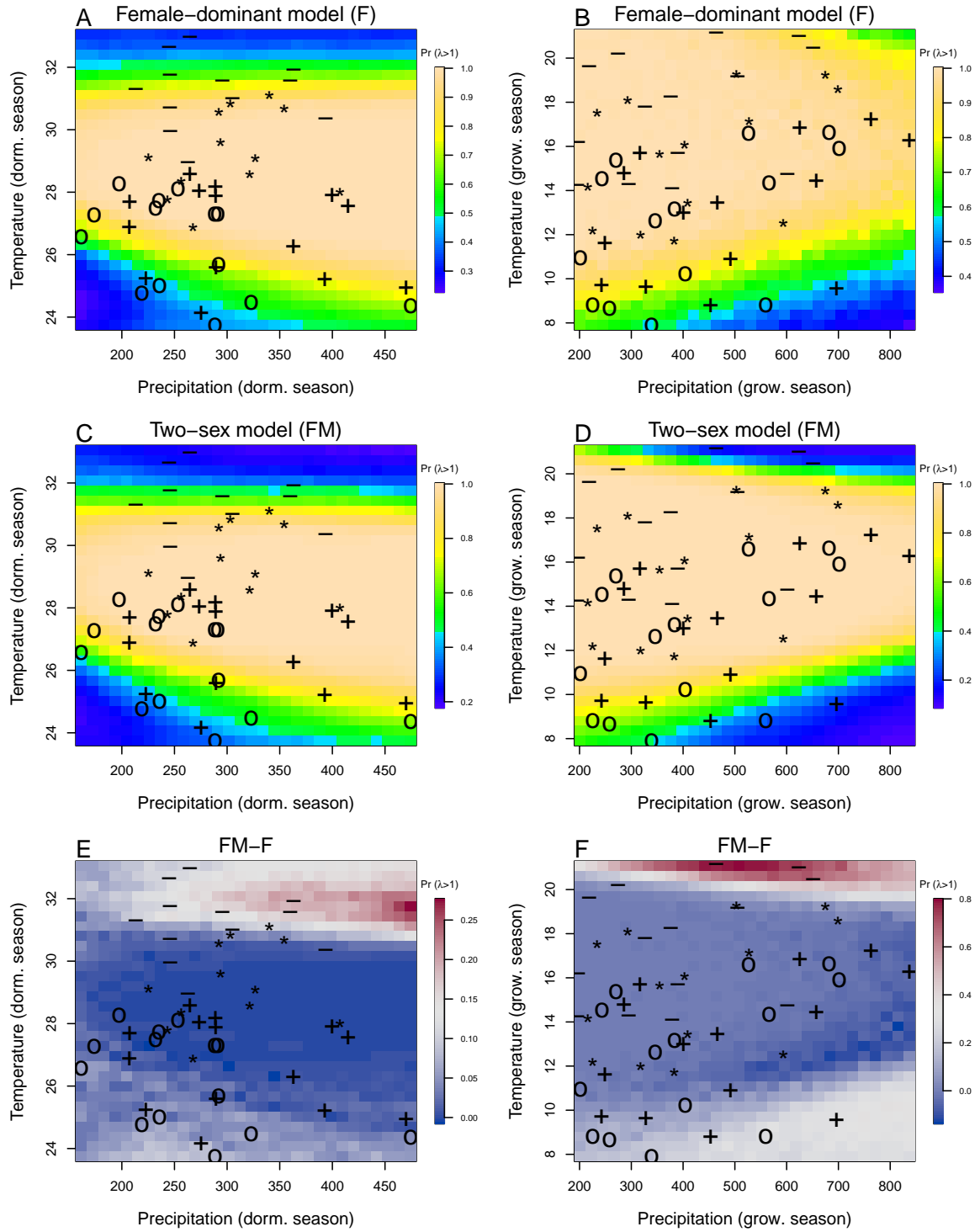


Figure 3: A two-dimensional representation of the predicted niche shift over time (past, present and future climate conditions). Contours on the first four panels show predicted probabilities of self-sustaining populations, $\text{Pr}(\lambda > 1)$ conditional on precipitation and temperature of the dormant and growing season. The last two panels show difference in niche estimation between the female dominant model and the two-sex model for each season. "○": Past, "+" Current, "*": RCP 4.5, "■": RCP 8.5.

361 **Climatic change induces shifts in geographic niche and population OSR**

362 Projecting the climatic niche onto geographic space, we find that suitable niche conditions for
363 Texas bluegrass are shifting north under climate change (Fig. 4). Under past (1901-1930) and
364 present (1990-2019) conditions, the two-sex and female-dominant models predict widespread
365 suitability with high confidence ($Pr(\lambda \geq 1) \approx 1$) across much of Texas and Oklahoma. For
366 both models, the predicted geographic niche generally corresponds well to independent
367 observations of the Texas bluegrass distribution (Fig.¹³). The predicted geographic niche is
368 more expansive than the observed distribution, particularly at southern, western, and eastern
369 edges, suggesting some degree of range disequilibrium (e.g., due to dispersal limitation),
370 geographic bias in occurrence observations, and/or model mis-specification. Comparing past
371 to present conditions, the geographic niche for both models has shifted slightly poleward,
372 with reductions in viability at the southern margins and expansions of viability at northern
373 margins. The northward shift of suitable niche conditions is even more pronounced in
374 projections to end-of-century (2071-2100) conditions, with the most dramatic changes in the
375 most pessimistic (RCP8.5) scenario (Fig.¹⁴). In fact, under the pessimistic scenario, Texas
376 bluegrass will have very little remaining climate suitability in the state of Texas by the end
377 of the 21st century. The predicted poleward niche shift is consistent across different global
378 circulation models (Figure S-15, Figure S-16, Figure S-17).

379 Female-dominant and two-sex models are in broad agreement about northward
380 migration of the climatic niche, but the geographic projections reveal hotspots of disagreement
381 where the female-dominant model over-predicts climate suitability and under-predicts the
382 likelihood of range shifts (Fig. 4). These hotspots are generally regions of predicted female
383 bias in the operational sex ratio (Fig. WE NEED A FIGURE FOR THIS.) The strongest contrast
384 between the two models is in the pessimistic climate change scenario (RCP8.5), where the
385 female-dominant model over-predicts population viability by ca. 25%¹⁵ across much of the
386 region (Fig. WE NEED A FIGURE SHOWING THE DISTRIBUTION OF THE DIFFERENCE)
387 and under-estimates the magnitude of a potential range shift. In this scenario, a broad swath
388 of the current distribution that is forecasted to be effectively unsuitable ($Pr(\lambda \geq 1) \approx 0$) by the
389 two-sex model is identified as marginally suitable ($Pr(\lambda \geq 1) \approx 0.5$) by the female-dominant
390 model. Accordingly, the OSR of Texas bluegrass across its range is projected to be ca. 75%
391 female panicles, on average, by end of century under RCP8.5, an increase from ca. 60% female
392 under projections for past and current conditions (Fig. 5). The more optimistic climate change
393 scenario (RCP4.5) predicts an intermediate shift in OSR, with hotspots of change becoming

¹³I think we should add the GBIF records to the map.

¹⁴Here and throughout, we need to reference specific figure panels by letter label.

¹⁵I just eyeballed this. Real number should come from the histograms.

³⁹⁴ strongly female-biased but most of the range remaining near current levels of 60% female
³⁹⁵ (Fig. 5; WE NEED A MAP SHOWING WHERE OSR IS BECOMING MORE BIASED).

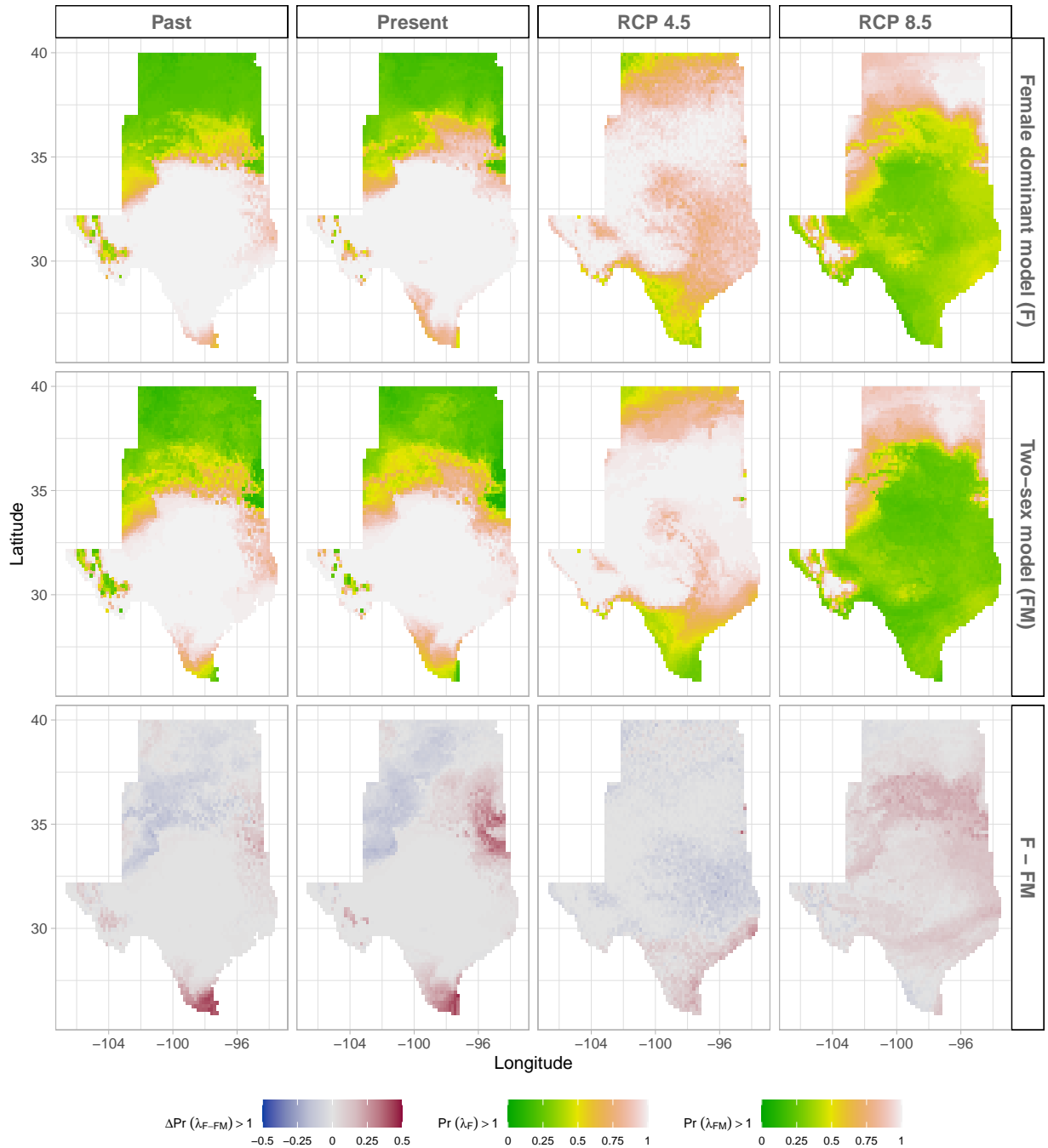


Figure 4: Climate change favors range shift towards north edge. (A) Past, (B) Current, (C and D) Future predicted range shift based on the predicted probabilities of self- sustaining populations, $\Pr(\lambda > 1)$, using the two-sex model that incorporates sex- specific demographic responses to climate with sex ratio dependent seed fertilization. (E) Past, (F) Current, (G and H) Future predicted range shift based on the predicted probabilities of self- sustaining populations, $\Pr(\lambda > 1)$, using the female dominant model. Future projections were based on the CMCC-CM model. The black dots on panel B and F indicate all known presence points collected from GBIF from 1990 to 2019, which corresponds to the current condition in our prediction. The occurrences of GBIFs are distributed in with higher population fitness habitat $\Pr(\lambda > 1)$, confirming that our study approach can reasonably predict range shifts.

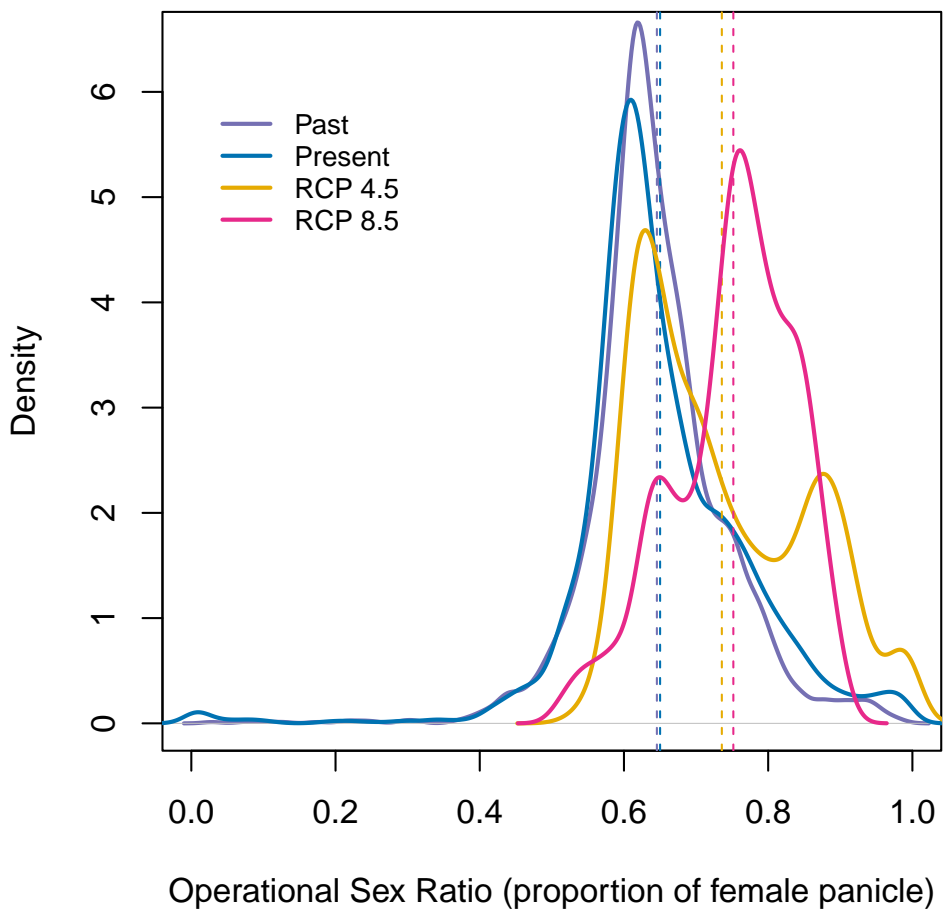


Figure 5: Change in Operational Sex Ratio (proportion of female panicle) over time (past, present, future). Future projections were based on the CMCC-CM model. The mean sex ratio for each time period is shown as vertical dashed line.

396 Discussion

397 Dioecious species make up a large fraction of Earth's biodiversity – most animals and many
 398 plants – yet we have little knowledge about how sex-specific demography and responses to
 399 climate drivers may affect population viability and range shifts of dioecious species under
 400 climate change.¹⁶ We used demographic data collected common garden experiments and
 401 sex-structured demographic modeling to forecast for the first time the likely impact of climate
 402 change on range dynamics of a dioecious species. Our future projections require extrapolation
 403 to warmer or colder conditions than observed in our experiment and subsequently should be

¹⁶*Love this opening sentence.*

404 interpreted with caution (Chen et al., 2024).¹⁷ Three general patterns emerged from our analysis
405 of range-wide common garden experiments and sex-structured, climate-explicit demographic
406 models. First, our Bayesian mixed effect model suggests a sex specific demographic response
407 to climate change that lead to higher proportion of female as climate increase. Second, climate
408 change favors a northern range shifts in suitable habitats. Third, the female dominant model
409 (model that does not account for sex structure) overestimates species niche and range shifts.

410 There was a female demographic advantage leading to a female biased in response
411 to climate change in *Poa arachnifera* populations. The extreme female-bias in response to
412 climate change contrast with previous studies suggesting that an increase in male frequency
413 in response to climate change (Hultine et al., 2016; Petry et al., 2016). Two mechanisms
414 could explain the observed demographic advantage of females over males for survival and
415 flowering and the opposite for growth and number of panicles. The trade-off between fitness
416 traits (survival, growth and fertility) due to resource limitation and the pollination mode of
417 our study species (wind pollinated) could explain such a result (Cipollini and Whigham, 1994;
418 Freeman et al., 1976). For most species, the cost of reproduction is often higher for females
419 than males due to the requirement to develop seeds and fruits (Hultine et al., 2016). However,
420 several studies reported a higher cost of reproduction for males in wind pollinated species
421 due to the larger amounts of pollen they produce (Bruijning et al., 2017; Bürli et al., 2022;
422 Cipollini and Whigham, 1994; Field et al., 2013).

423 Our results suggest that climate change will alter population at the center of the range
424 and drive a northern range shifts. This impact of climate change on the species current
425 niche could be explained by the increase of temperature over the next years. Small change
426 in temperature of the growing and dormant season have a larger impact on population
427 viability. Temperature can impact plant populations through different mechanisms. Increasing
428 temperature could increase evaporative demand, affect plant phenology (Iler et al., 2019;
429 McLean et al., 2016; Sherry et al., 2007), and germination rate (Reed et al., 2021). The potential
430 for temperature to influence these different processes changes seasonally (Konapala et al.,
431 2020). For example, studies suggested that species that are active during the growing season
432 such as cool grass species can have delayed phenology in response to global warming,
433 particularly if temperatures rise above their physiological tolerances (Cleland et al., 2007;
434 Williams et al., 2015). In addition, high temperature during the growing season by affecting
435 pollen viability, fertilization could affect seed formation and germination (Hatfield and
436 Prueger, 2015; Sletvold and Ågren, 2015). Pollen dispersal may allow plants to resist climate
437 change because pollen dispersal may provide the local genetic diversity necessary to adapt
438 at the leading edge of the population (Corlett and Westcott, 2013; Duputié et al., 2012; Kremer

¹⁷ I think extrapolation should be its own paragraph. This also relates to uncertainty in the climate forecasts.

et al., 2012). Since wind pollination is most effective at short distances, it is most often found in plant species growing at high density such as our study species, it is less likely that dispersal limitation affect niche shift in our study system. Difference in non-climatic factors such as soil, or biotic interactions could also explain decline in population growth rate as an indirect effects of increase in temperature (Alexander et al., 2015; Schultz et al., 2022). For example, climate change could increase the strength of species competition and thereby constrain our study species to a narrower realized niche (Aguilée et al., 2016; Pulliam, 2000).

We found evidence of underestimation of the impact of climatic change on population dynamics by the female dominant model and implication for such an underestimation on conservation actions for dioecious species. The underestimation of the impact of climatic change on population dynamics by the female dominant model makes sense given the sex specific response to climatic change. *Poa arachnifera* populations will be female biased in response to climate change. That extreme female-bias could affect population growth rate by altering males' fitness with reduction on mate availability given that females individuals have a demographic advantage over males (Haridas et al., 2014; Knight et al., 2005). Further, our work suggest that population viability is sensitive to climate under current and future conditions. This is key because most conservation actions are design from data on current responses to climate, rather than future response to climate (Sletvold et al., 2013). Since the role of male is not negligible in accuralrtly predicting dioecious species response to climate change, management strategies that focus on both sexes would be effective and will enhance our understanding of dioecious species response to global warming.

Conclusion

We have investigated the potential consequence of skewness in sex ratio on population dynamics and range shift in the context of climate change using the Texas bluegrass. We found extreme female -biased in response to climate change. The effect of female biased will induce range shifts to the northern edge of the species current range by limiting mate availability. Beyond, our study case, our results also suggest that tracking only one sex could lead to an underestimation of the effect of climate change on population dynamics. Our work provides also a framework for predicting the impact of global warming on population dynamics using the probability of population to self-sustain.

⁴⁶⁹ **Acknowledgements**

⁴⁷⁰ This research was supported by National Science Foundation Division of Environmental
⁴⁷¹ Biology awards 2208857 and 2225027. We thank the institutions who hosted us at their field
⁴⁷² station facilities, including

473 **References**

- 474 Aguilée, R., Raoul, G., Rousset, F., and Ronce, O. (2016). Pollen dispersal slows geographical
475 range shift and accelerates ecological niche shift under climate change. *Proceedings of the*
476 *National Academy of Sciences*, 113(39):E5741–E5748.
- 477 Alexander, J. M., Diez, J. M., and Levine, J. M. (2015). Novel competitors shape species'
478 responses to climate change. *Nature*, 525(7570):515–518.
- 479 Bertrand, R., Lenoir, J., Piedallu, C., Riofrío-Dillon, G., De Ruffray, P., Vidal, C., Pierrat, J.-C.,
480 and Gégout, J.-C. (2011). Changes in plant community composition lag behind climate
481 warming in lowland forests. *Nature*, 479(7374):517–520.
- 482 Bruijning, M., Visser, M. D., Muller-Landau, H. C., Wright, S. J., Comita, L. S., Hubbell, S. P.,
483 de Kroon, H., and Jongejans, E. (2017). Surviving in a cosexual world: A cost-benefit
484 analysis of dioecy in tropical trees. *The American Naturalist*, 189(3):297–314.
- 485 Bürli, S., Pannell, J. R., and Tonnabel, J. (2022). Environmental variation in sex ratios and
486 sexual dimorphism in three wind-pollinated dioecious plant species. *Oikos*, 2022(6):e08651.
- 487 Bürkner, P.-C. (2017). brms: An R package for Bayesian multilevel models using Stan. *Journal*
488 *of Statistical Software*, 80(1):1–28.
- 489 Caswell, H. (1989). Analysis of life table response experiments i. decomposition of effects
490 on population growth rate. *Ecological Modelling*, 46(3-4):221–237.
- 491 Caswell, H. (2000). *Matrix population models*, volume 1. Sinauer Sunderland, MA.
- 492 Chen, X., Liang, Y., and Feng, X. (2024). Influence of model complexity, training collinearity,
493 collinearity shift, predictor novelty and their interactions on ecological forecasting. *Global*
494 *Ecology and Biogeography*, 33(3):371–384.
- 495 Cipollini, M. L. and Whigham, D. F. (1994). Sexual dimorphism and cost of reproduction
496 in the dioecious shrub *lindera benzoin* (lauraceae). *American Journal of Botany*, 81(1):65–75.
- 497 Cleland, E. E., Chuine, I., Menzel, A., Mooney, H. A., and Schwartz, M. D. (2007). Shifting
498 plant phenology in response to global change. *Trends in ecology & evolution*, 22(7):357–365.
- 499 Compagnoni, A., Steigman, K., and Miller, T. E. (2017). Can't live with them, can't live
500 without them? balancing mating and competition in two-sex populations. *Proceedings of*
501 *the Royal Society B: Biological Sciences*, 284(1865):20171999.

- 502 Corlett, R. T. and Westcott, D. A. (2013). Will plant movements keep up with climate change?
503 *Trends in ecology & evolution*, 28(8):482–488.
- 504 Czachura, K. and Miller, T. E. (2020). Demographic back-casting reveals that subtle
505 dimensions of climate change have strong effects on population viability. *Journal of Ecology*,
506 108(6):2557–2570.
- 507 Dahlgren, J. P., Bengtsson, K., and Ehrlén, J. (2016). The demography of climate-driven and
508 density-regulated population dynamics in a perennial plant. *Ecology*, 97(4):899–907.
- 509 Davis, M. B. and Shaw, R. G. (2001). Range shifts and adaptive responses to quaternary
510 climate change. *Science*, 292(5517):673–679.
- 511 Diez, J. M., Giladi, I., Warren, R., and Pulliam, H. R. (2014). Probabilistic and spatially variable
512 niches inferred from demography. *Journal of ecology*, 102(2):544–554.
- 513 Duputié, A., Massol, F., Chuine, I., Kirkpatrick, M., and Ronce, O. (2012). How do genetic cor-
514 relations affect species range shifts in a changing environment? *Ecology letters*, 15(3):251–259.
- 515 Eberhart-Phillips, L. J., Küpper, C., Miller, T. E., Cruz-López, M., Maher, K. H., Dos Remedios,
516 N., Stoffel, M. A., Hoffman, J. I., Krüger, O., and Székely, T. (2017). Sex-specific early
517 survival drives adult sex ratio bias in snowy plovers and impacts mating system and
518 population growth. *Proceedings of the National Academy of Sciences*, 114(27):E5474–E5481.
- 519 Ehrlén, J. and Morris, W. F. (2015). Predicting changes in the distribution and abundance
520 of species under environmental change. *Ecology letters*, 18(3):303–314.
- 521 Elderd, B. D. and Miller, T. E. (2016). Quantifying demographic uncertainty: Bayesian methods
522 for integral projection models. *Ecological Monographs*, 86(1):125–144.
- 523 Ellis, R. P., Davison, W., Queirós, A. M., Kroeker, K. J., Calosi, P., Dupont, S., Spicer, J. I.,
524 Wilson, R. W., Widdicombe, S., and Urbina, M. A. (2017). Does sex really matter? explaining
525 intraspecies variation in ocean acidification responses. *Biology letters*, 13(2):20160761.
- 526 Ellner, S. P., Adler, P. B., Childs, D. Z., Hooker, G., Miller, T. E., and Rees, M. (2022). A critical
527 comparison of integral projection and matrix projection models for demographic analysis:
528 Comment. *Ecology*.
- 529 Ellner, S. P., Childs, D. Z., Rees, M., et al. (2016). Data-driven modelling of structured
530 populations. *A practical guide to the Integral Projection Model*. Cham: Springer.

- 531 Evans, M. E., Merow, C., Record, S., McMahon, S. M., and Enquist, B. J. (2016). Towards
532 process-based range modeling of many species. *Trends in Ecology & Evolution*, 31(11):860–871.
- 533 Field, D. L., Pickup, M., and Barrett, S. C. (2013). Comparative analyses of sex-ratio variation
534 in dioecious flowering plants. *Evolution*, 67(3):661–672.
- 535 Freeman, D. C., Klikoff, L. G., and Harper, K. T. (1976). Differential resource utilization by
536 the sexes of dioecious plants. *Science*, 193(4253):597–599.
- 537 Gamelon, M., Grøtan, V., Nilsson, A. L., Engen, S., Hurrell, J. W., Jerstad, K., Phillips, A. S.,
538 Røstad, O. W., Slagsvold, T., Walseng, B., et al. (2017). Interactions between demography
539 and environmental effects are important determinants of population dynamics. *Science
540 Advances*, 3(2):e1602298.
- 541 Gerber, L. R. and White, E. R. (2014). Two-sex matrix models in assessing population viability:
542 when do male dynamics matter? *Journal of Applied Ecology*, 51(1):270–278.
- 543 Gissi, E., Bowyer, R. T., and Bleich, V. C. (2024). Sex-based differences affect conservation.
544 *Science*, 384(6702):1309–1310.
- 545 Gissi, E., Schiebinger, L., Hadly, E. A., Crowder, L. B., Santoleri, R., and Micheli, F. (2023).
546 Exploring climate-induced sex-based differences in aquatic and terrestrial ecosystems to
547 mitigate biodiversity loss. *nature communications*, 14(1):4787.
- 548 Haridas, C., Eager, E. A., Rebarber, R., and Tenhumberg, B. (2014). Frequency-dependent
549 population dynamics: Effect of sex ratio and mating system on the elasticity of population
550 growth rate. *Theoretical Population Biology*, 97:49–56.
- 551 Hatfield, J. and Prueger, J. (2015). Temperature extremes: effect on plant growth and
552 development. *weather clim extrem* 10: 4–10.
- 553 Hernández, C. M., Ellner, S. P., Adler, P. B., Hooker, G., and Snyder, R. E. (2023). An exact
554 version of life table response experiment analysis, and the r package exactltre. *Methods
555 in Ecology and Evolution*, 14(3):939–951.
- 556 Hitchcock, A. S. (1971). *Manual of the grasses of the United States*, volume 2. Courier Corporation.
- 557 Hultine, K. R., Grady, K. C., Wood, T. E., Shuster, S. M., Stella, J. C., and Whitham, T. G. (2016).
558 Climate change perils for dioecious plant species. *Nature Plants*, 2(8):1–8.

- 559 Iler, A. M., Compagnoni, A., Inouye, D. W., Williams, J. L., CaraDonna, P. J., Anderson, A., and
560 Miller, T. E. (2019). Reproductive losses due to climate change-induced earlier flowering are
561 not the primary threat to plant population viability in a perennial herb. *Journal of Ecology*,
562 107(4):1931–1943.
- 563 Jones, M. H., Macdonald, S. E., and Henry, G. H. (1999). Sex-and habitat-specific responses
564 of a high arctic willow, *salix arctica*, to experimental climate change. *Oikos*, pages 129–138.
- 565 Karger, D. N., Conrad, O., Böhner, J., Kawohl, T., Kreft, H., Soria-Auza, R. W., Zimmermann,
566 N. E., Linder, H. P., and Kessler, M. (2017). Climatologies at high resolution for the earth's
567 land surface areas. *Scientific data*, 4(1):1–20.
- 568 Kindiger, B. (2004). Interspecific hybrids of *poa arachnifera* × *poa secunda*. *Journal of New
569 Seeds*, 6(1):1–26.
- 570 Knight, T. M., Steets, J. A., Vamosi, J. C., Mazer, S. J., Burd, M., Campbell, D. R., Dudash,
571 M. R., Johnston, M. O., Mitchell, R. J., and Ashman, T.-L. (2005). Pollen limitation of plant
572 reproduction: pattern and process. *Annu. Rev. Ecol. Evol. Syst.*, 36:467–497.
- 573 Konapala, G., Mishra, A. K., Wada, Y., and Mann, M. E. (2020). Climate change will affect
574 global water availability through compounding changes in seasonal precipitation and
575 evaporation. *Nature communications*, 11(1):3044.
- 576 Kremer, A., Ronce, O., Robledo-Arnuncio, J. J., Guillaume, F., Bohrer, G., Nathan, R., Bridle,
577 J. R., Gomulkiewicz, R., Klein, E. K., Ritland, K., et al. (2012). Long-distance gene flow and
578 adaptation of forest trees to rapid climate change. *Ecology letters*, 15(4):378–392.
- 579 Lee-Yaw, J. A., Kharouba, H. M., Bontrager, M., Mahony, C., Csergő, A. M., Noreen, A. M.,
580 Li, Q., Schuster, R., and Angert, A. L. (2016). A synthesis of transplant experiments and
581 ecological niche models suggests that range limits are often niche limits. *Ecology letters*,
582 19(6):710–722.
- 583 Liaw, A., Wiener, M., et al. (2002). Classification and regression by randomforest. *R news*,
584 2(3):18–22.
- 585 Louthan, A. M., Keighron, M., Kiekebusch, E., Cayton, H., Terando, A., and Morris, W. F.
586 (2022). Climate change weakens the impact of disturbance interval on the growth rate of
587 natural populations of venus flytrap. *Ecological Monographs*, 92(4):e1528.

- 588 Lynch, H. J., Rhainds, M., Calabrese, J. M., Cantrell, S., Cosner, C., and Fagan, W. F. (2014).
589 How climate extremes—not means—define a species' geographic range boundary via a
590 demographic tipping point. *Ecological Monographs*, 84(1):131–149.
- 591 McLean, N., Lawson, C. R., Leech, D. I., and van de Pol, M. (2016). Predicting when climate-
592 driven phenotypic change affects population dynamics. *Ecology Letters*, 19(6):595–608.
- 593 Merow, C., Bois, S. T., Allen, J. M., Xie, Y., and Silander Jr, J. A. (2017). Climate change both
594 facilitates and inhibits invasive plant ranges in new england. *Proceedings of the National
595 Academy of Sciences*, 114(16):E3276–E3284.
- 596 Miller, T. and Compagnoni, A. (2022a). Data from: Two-sex demography, sexual niche
597 differentiation, and the geographic range limits of texas bluegrass (*Poa arachnifera*). *American
598 Naturalist, Dryad Digital Repository*,. <https://doi.org/10.5061/dryad.kkwh70s5x>.
- 599 Miller, T. E. and Compagnoni, A. (2022b). Two-sex demography, sexual niche differentiation,
600 and the geographic range limits of texas bluegrass (*poa arachnifera*). *The American
601 Naturalist*, 200(1):17–31.
- 602 Miller, T. E., Shaw, A. K., Inouye, B. D., and Neubert, M. G. (2011). Sex-biased dispersal and
603 the speed of two-sex invasions. *The American Naturalist*, 177(5):549–561.
- 604 Morrison, C. A., Robinson, R. A., Clark, J. A., and Gill, J. A. (2016). Causes and consequences
605 of spatial variation in sex ratios in a declining bird species. *Journal of Animal Ecology*,
606 85(5):1298–1306.
- 607 Pease, C. M., Lande, R., and Bull, J. (1989). A model of population growth, dispersal and
608 evolution in a changing environment. *Ecology*, 70(6):1657–1664.
- 609 Petry, W. K., Soule, J. D., Iler, A. M., Chicas-Mosier, A., Inouye, D. W., Miller, T. E., and
610 Mooney, K. A. (2016). Sex-specific responses to climate change in plants alter population
611 sex ratio and performance. *Science*, 353(6294):69–71.
- 612 Piironen, J. and Vehtari, A. (2017). Comparison of bayesian predictive methods for model
613 selection. *Statistics and Computing*, 27:711–735.
- 614 Pottier, P., Burke, S., Drobniak, S. M., Lagisz, M., and Nakagawa, S. (2021). Sexual (in) equality?
615 a meta-analysis of sex differences in thermal acclimation capacity across ectotherms.
616 *Functional Ecology*, 35(12):2663–2678.

- 617 Pulliam, H. R. (2000). On the relationship between niche and distribution. *Ecology letters*,
618 3(4):349–361.
- 619 R Core Team (2023). *R: A Language and Environment for Statistical Computing*. R Foundation
620 for Statistical Computing, Vienna, Austria.
- 621 Reed, P. B., Peterson, M. L., Pfeifer-Meister, L. E., Morris, W. F., Doak, D. F., Roy, B. A., Johnson,
622 B. R., Bailes, G. T., Nelson, A. A., and Bridgman, S. D. (2021). Climate manipulations
623 differentially affect plant population dynamics within versus beyond northern range limits.
624 *Journal of Ecology*, 109(2):664–675.
- 625 Renganayaki, K., Jessup, R., Burson, B., Hussey, M., and Read, J. (2005). Identification of
626 male-specific AFLP markers in dioecious Texas bluegrass. *Crop science*, 45(6):2529–2539.
- 627 Sanderson, B. M., Knutti, R., and Caldwell, P. (2015). A representative democracy to reduce
628 interdependency in a multimodel ensemble. *Journal of Climate*, 28(13):5171–5194.
- 629 Schultz, E. L., Hülsmann, L., Pillet, M. D., Hartig, F., Breshears, D. D., Record, S., Shaw, J. D.,
630 DeRose, R. J., Zuidema, P. A., and Evans, M. E. (2022). Climate-driven, but dynamic and
631 complex? a reconciliation of competing hypotheses for species' distributions. *Ecology letters*,
632 25(1):38–51.
- 633 Schwalm, C. R., Glendon, S., and Duffy, P. B. (2020). Rcp8.5 tracks cumulative CO₂ emissions.
634 *Proceedings of the National Academy of Sciences*, 117(33):19656–19657.
- 635 Schwinning, S., Lortie, C. J., Esque, T. C., and DeFalco, L. A. (2022). What common-garden
636 experiments tell us about climate responses in plants.
- 637 Sexton, J. P., McIntyre, P. J., Angert, A. L., and Rice, K. J. (2009). Evolution and ecology of
638 species range limits. *Annu. Rev. Ecol. Evol. Syst.*, 40:415–436.
- 639 Shelton, A. O. (2010). The ecological and evolutionary drivers of female-biased sex ratios:
640 two-sex models of perennial seagrasses. *The American Naturalist*, 175(3):302–315.
- 641 Sherry, R. A., Zhou, X., Gu, S., Arnone III, J. A., Schimel, D. S., Verburg, P. S., Wallace,
642 L. L., and Luo, Y. (2007). Divergence of reproductive phenology under climate warming.
643 *Proceedings of the National Academy of Sciences*, 104(1):198–202.
- 644 Sletvold, N. and Ågren, J. (2015). Climate-dependent costs of reproduction: Survival and
645 fecundity costs decline with length of the growing season and summer temperature.
646 *Ecology Letters*, 18(4):357–364.

- 647 Sletvold, N., Dahlgren, J. P., Øien, D.-I., Moen, A., and Ehrlén, J. (2013). Climate warming
648 alters effects of management on population viability of threatened species: results from
649 a 30-year experimental study on a rare orchid. *Global Change Biology*, 19(9):2729–2738.
- 650 Smith, M. D., Wilkins, K. D., Holdrege, M. C., Wilfahrt, P., Collins, S. L., Knapp, A. K., Sala,
651 O. E., Dukes, J. S., Phillips, R. P., Yahdjian, L., et al. (2024). Extreme drought impacts have
652 been underestimated in grasslands and shrublands globally. *Proceedings of the National
653 Academy of Sciences*, 121(4):e2309881120.
- 654 Stan Development Team (2023). RStan: the R interface to Stan. R package version 2.21.8.
- 655 Thomson, A. M., Calvin, K. V., Smith, S. J., Kyle, G. P., Volke, A., Patel, P., Delgado-Arias,
656 S., Bond-Lamberty, B., Wise, M. A., Clarke, L. E., et al. (2011). Rcp4. 5: a pathway for
657 stabilization of radiative forcing by 2100. *Climatic change*, 109:77–94.
- 658 Tognetti, R. (2012). Adaptation to climate change of dioecious plants: does gender balance
659 matter? *Tree Physiology*, 32(11):1321–1324.
- 660 Williams, J. L., Jacquemyn, H., Ochocki, B. M., Brys, R., and Miller, T. E. (2015). Life
661 history evolution under climate change and its influence on the population dynamics of
662 a long-lived plant. *Journal of Ecology*, 103(4):798–808.

Supporting Information

663 S.1 Supporting Figures

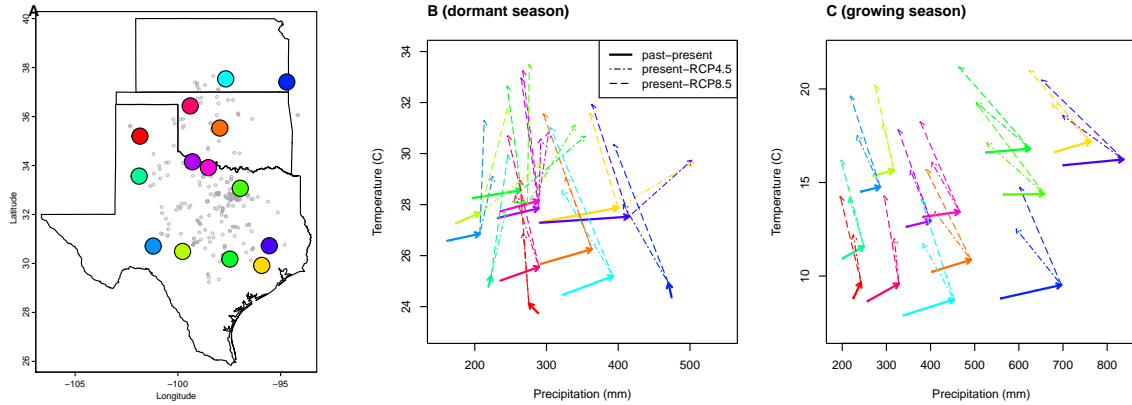


Figure S-1: (A), Common garden locations in Texas, Oklahoma, and Kansas (points) and (B,C) corresponding changes in growing and dormant season climate. Arrows in B,C connect past (1901-1930) and present (1990-2019) climate normals, and present and future (2071-2100) climate normals under RCP4.5 and RCP8.5 forecasts. Future forecasts are from MIROC5 but other climate models show similar patterns.

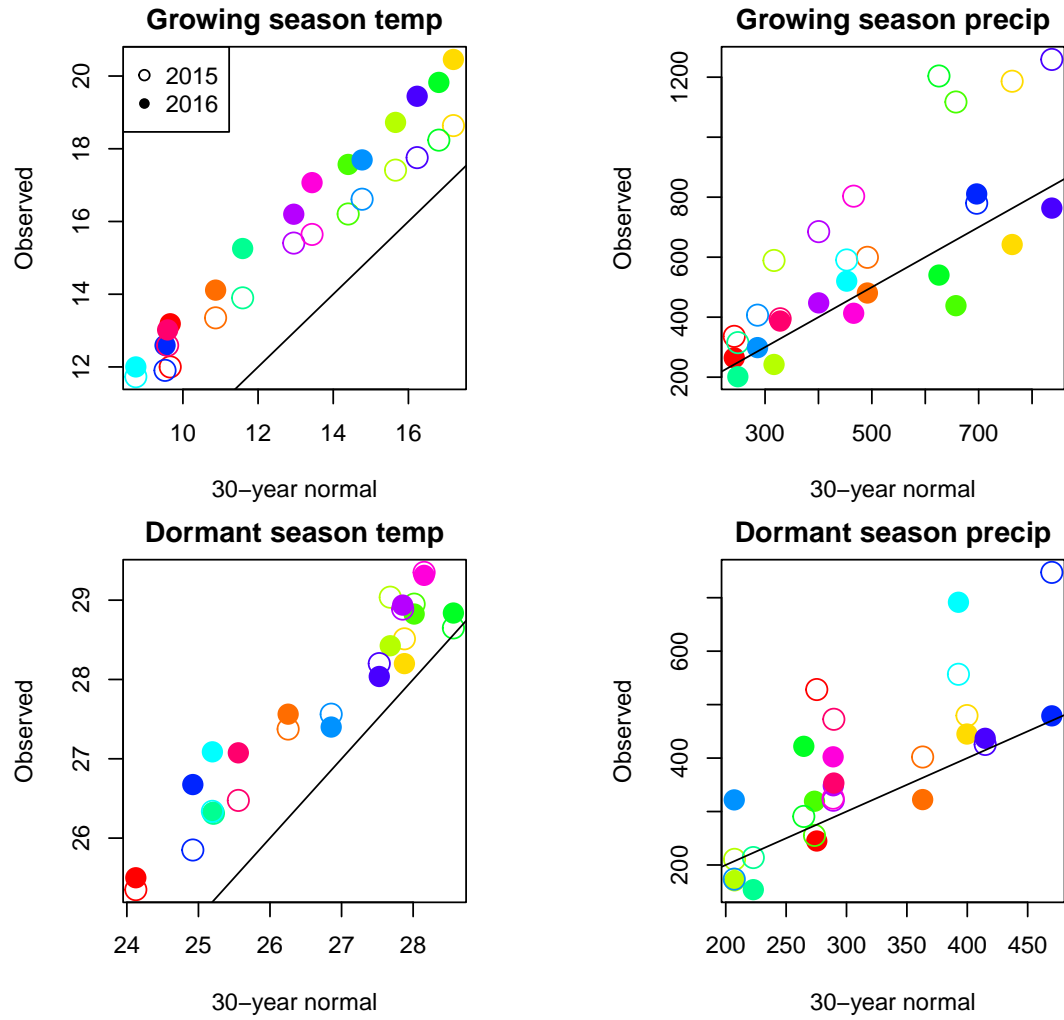


Figure S-2: Comparison of 30-year (1990-2019) climate normals and observed weather conditions at common garden sites during the 2014–15 and 2015–16 census periods. Temperature is in $^{\circ}\text{C}$ and precipitation is in mm . Colors represent sites and lines show the $y=x$ relationship.

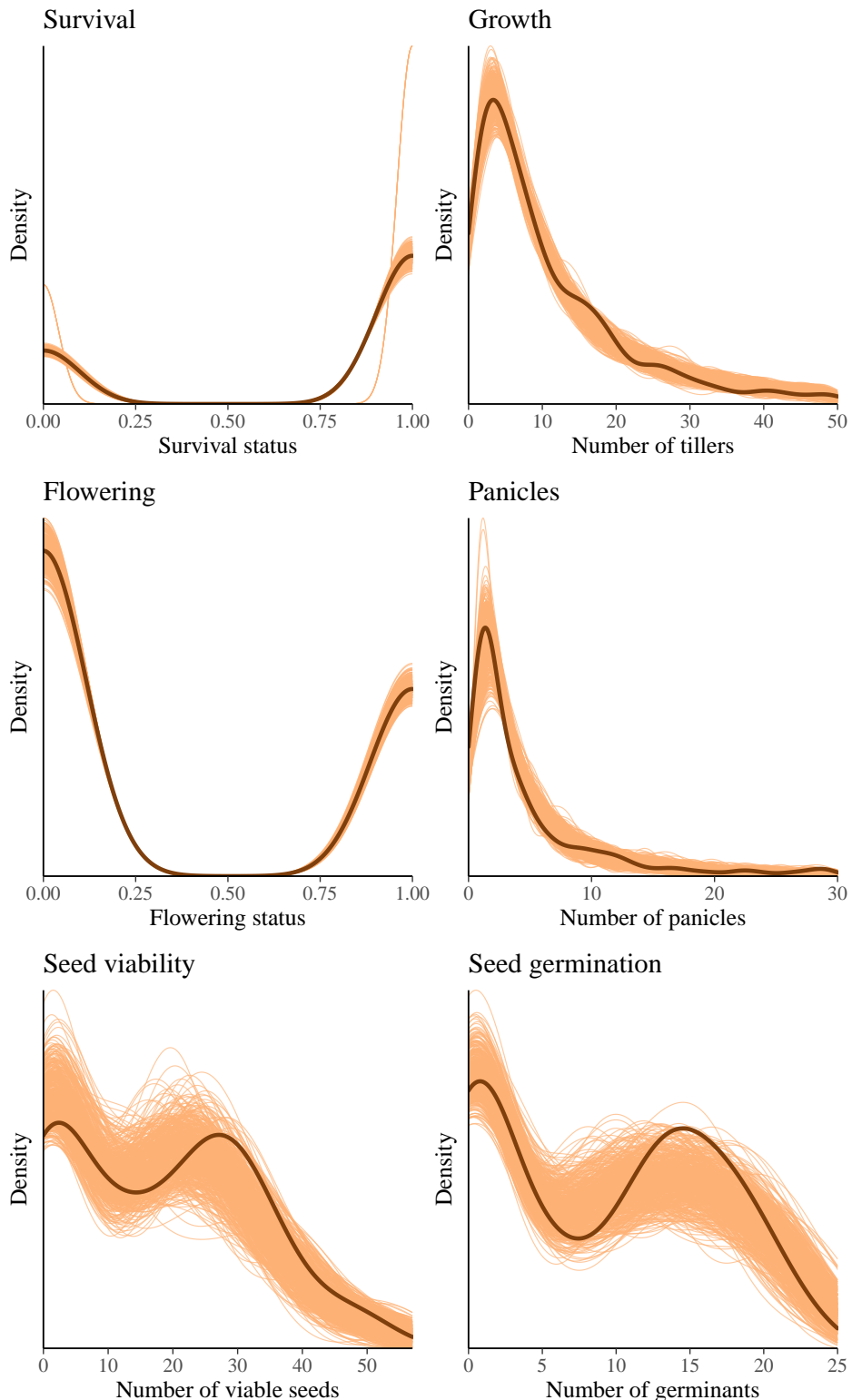


Figure S-3: Posterior predictive checks. Consistency between real data and simulated values suggests that the fitted vital rate models accurately describes the data. Graph shows density curves for the observed data (light orange) along with the simulated values (dark orange).

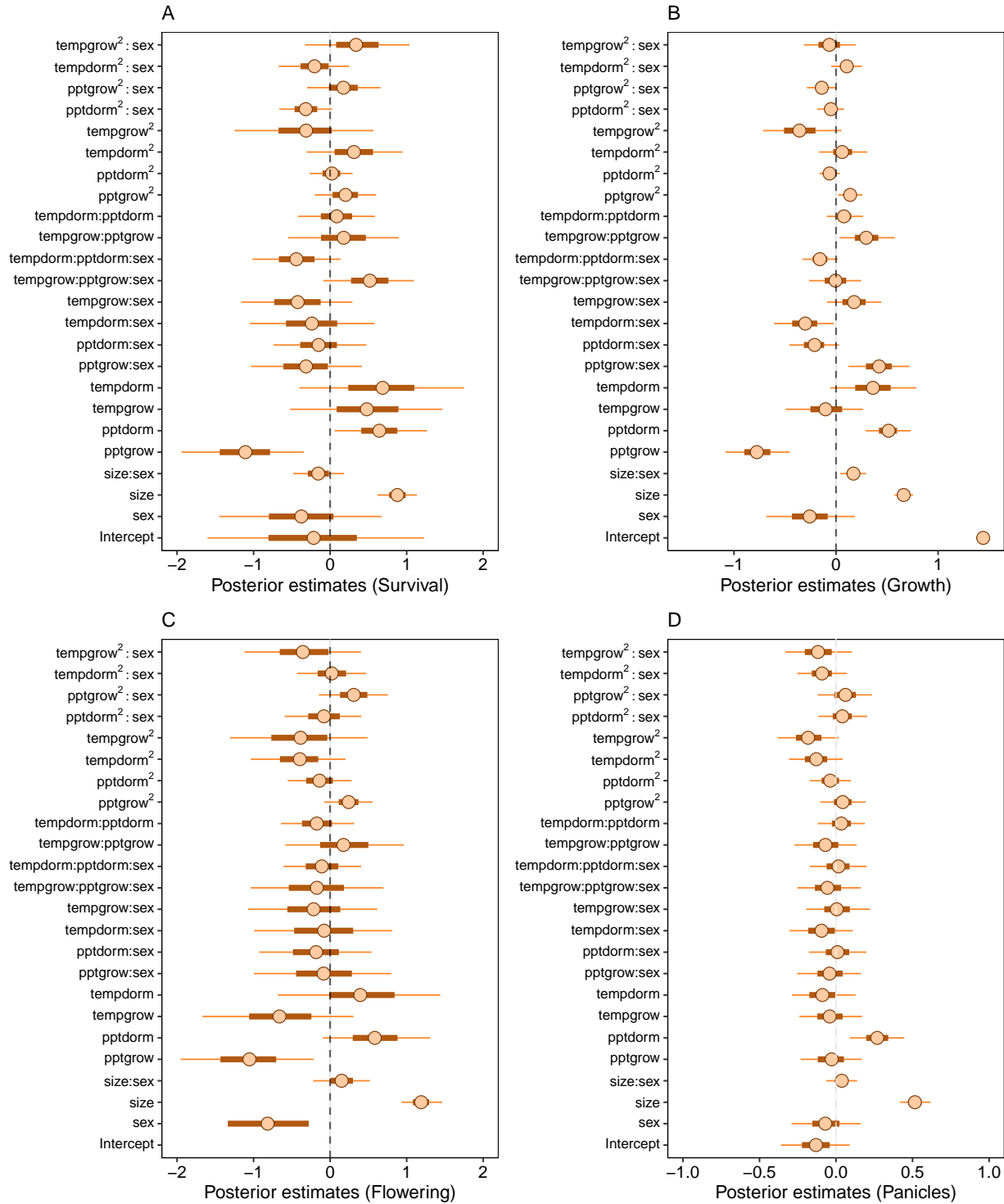


Figure S-4: Mean parameter values and 95% credible intervals of the posterior probability distributions. pptgrow is the precipitation of growing season, Tempgrow is the temperature of growing season, pptdorm is the temperature of dormant season, Tempdorm is the temperature of dormant season.

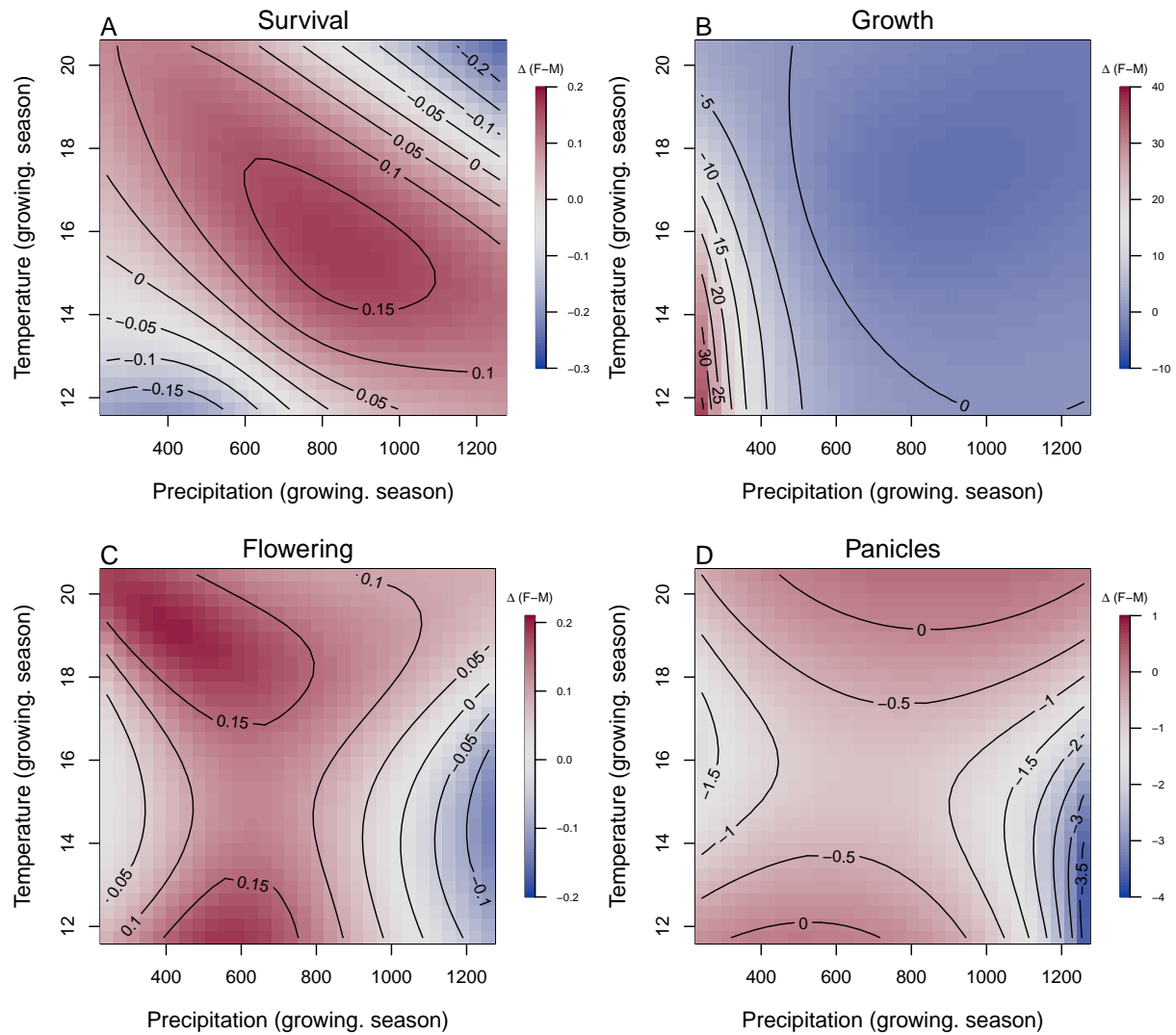


Figure S-5: Predicted difference in demographic response to climate across species range between female and male. Contours show predicted value of that difference conditional on precipitation and temperature of growing season

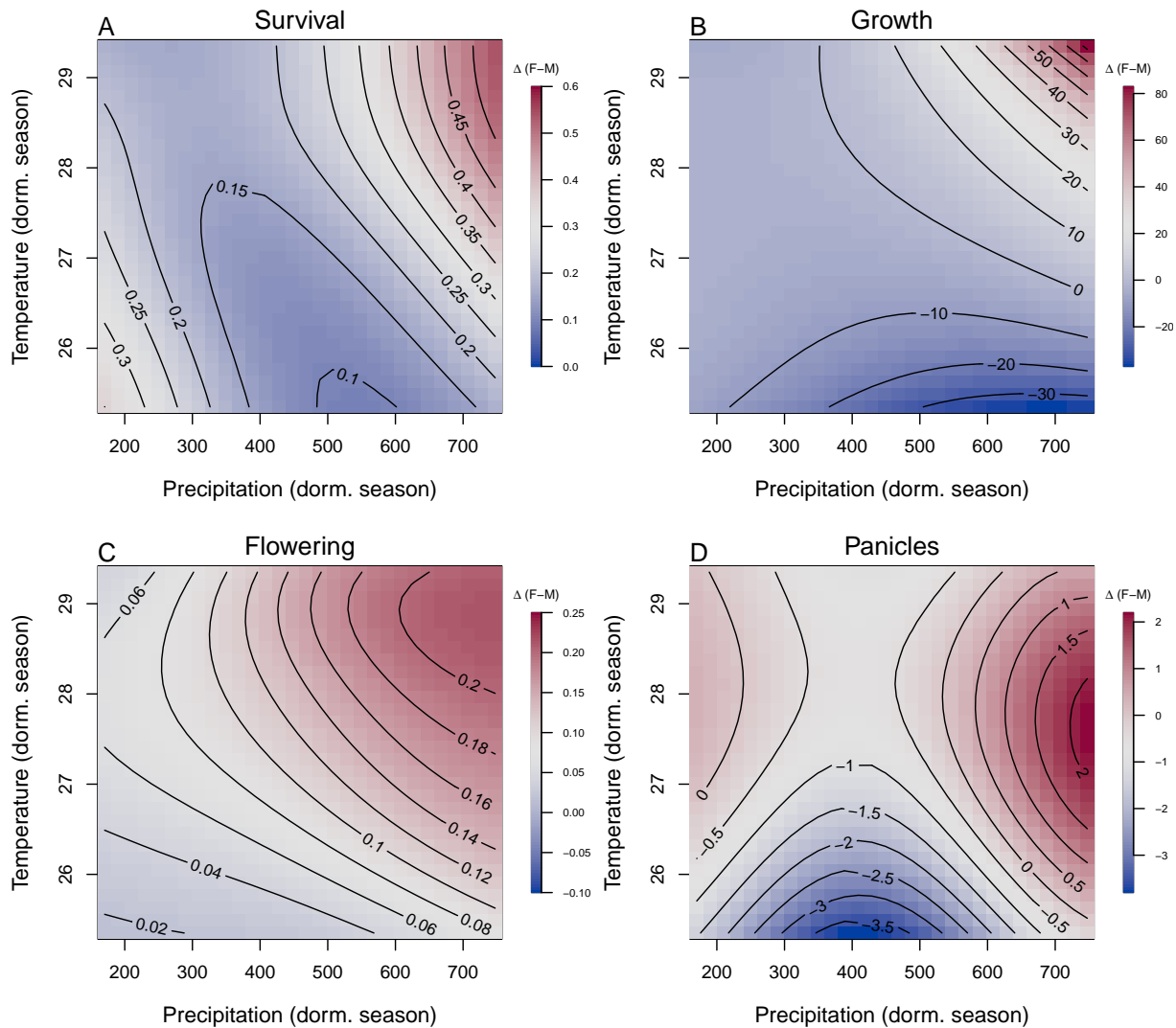


Figure S-6: Predicted difference in demographic response to climate across species range between female and male. Contours show predicted value of that difference conditional on precipitation and temperature of the dormant season

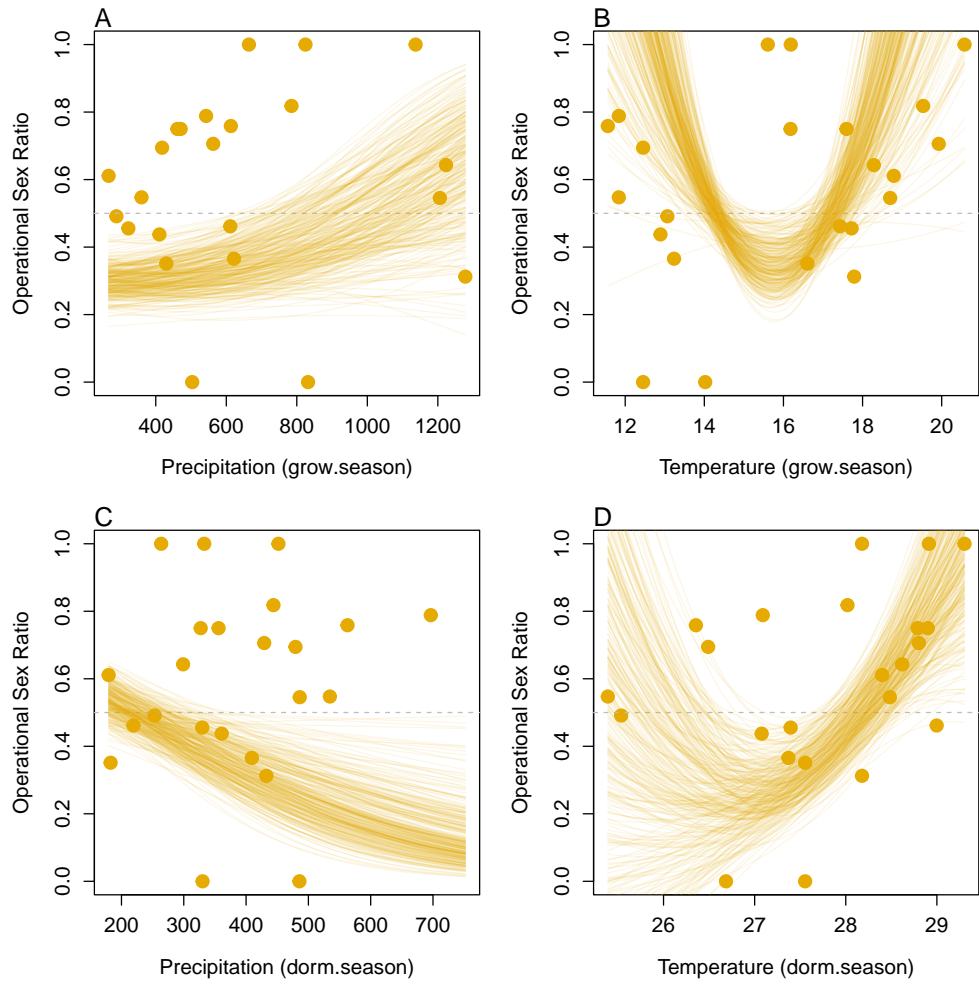


Figure S-7: Significant Operational Sex Ratio response across climate gradient. (A, B) Proportion of panicles that were females across precipitation and temperature of the growing season; (C, D) Proportion of panicles that were females across precipitation and temperature of the dormant season.

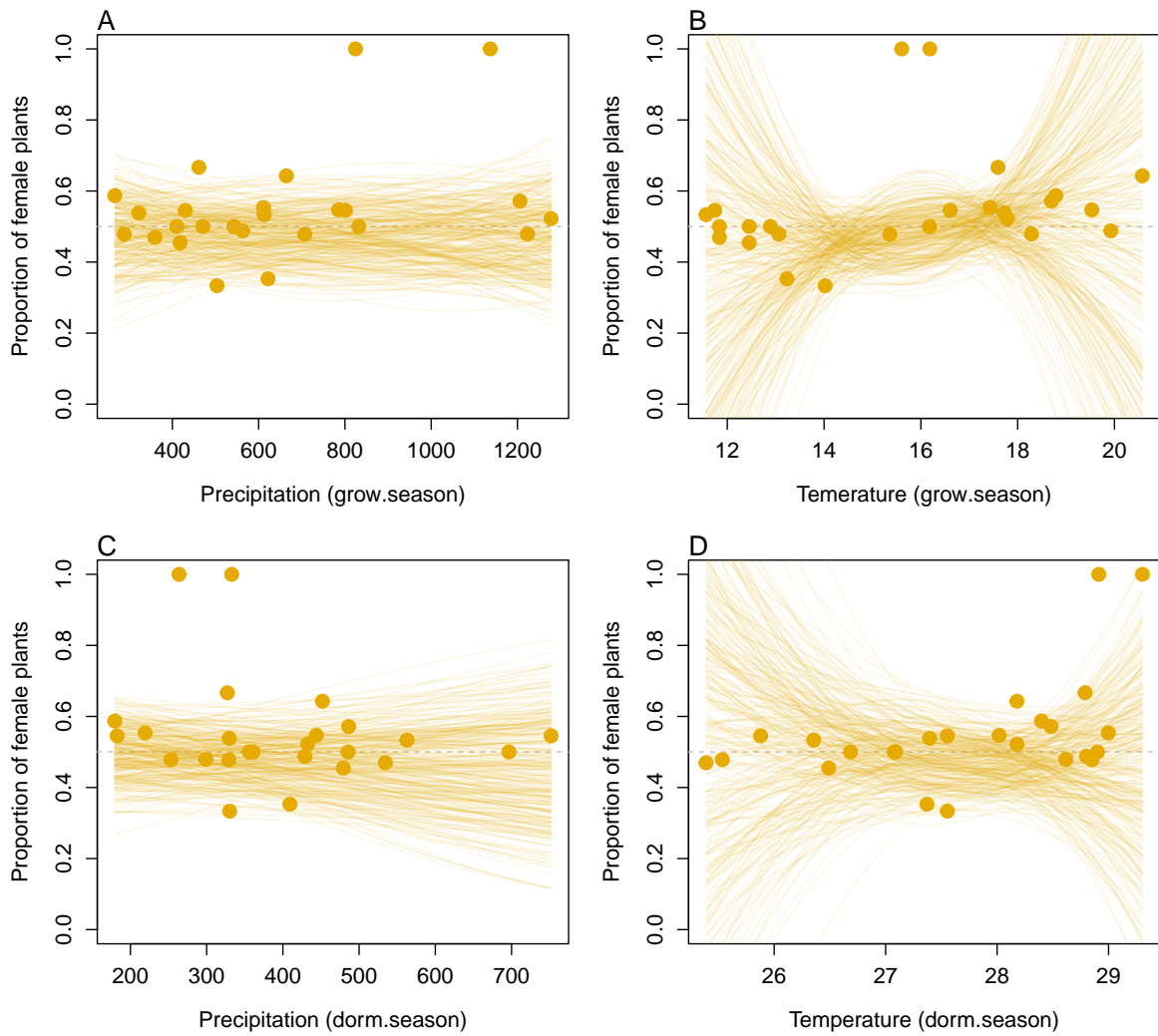


Figure S-8: Variation in sex-ratio accross climate gradient. (A, B) Proportion of plants that were females across precipitation and temperature of the growing season; (C, D) Proportion of plants that were females across precipitation and temperature of the dormant season.

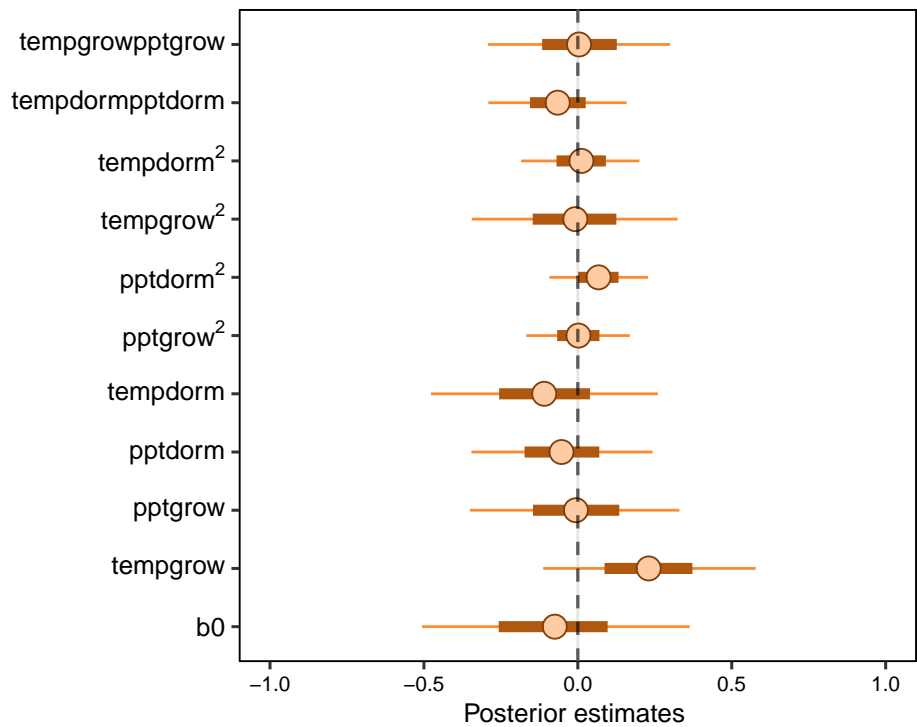


Figure S-9: Mean parameter values and 95% credible intervals of the posterior probability distributions. pptgrow is the precipitation of growing season, Tempgrow is the temperature of growing season, pptdorm is the temperature of dormant season, Tempdorm is the temperature of dormant season.

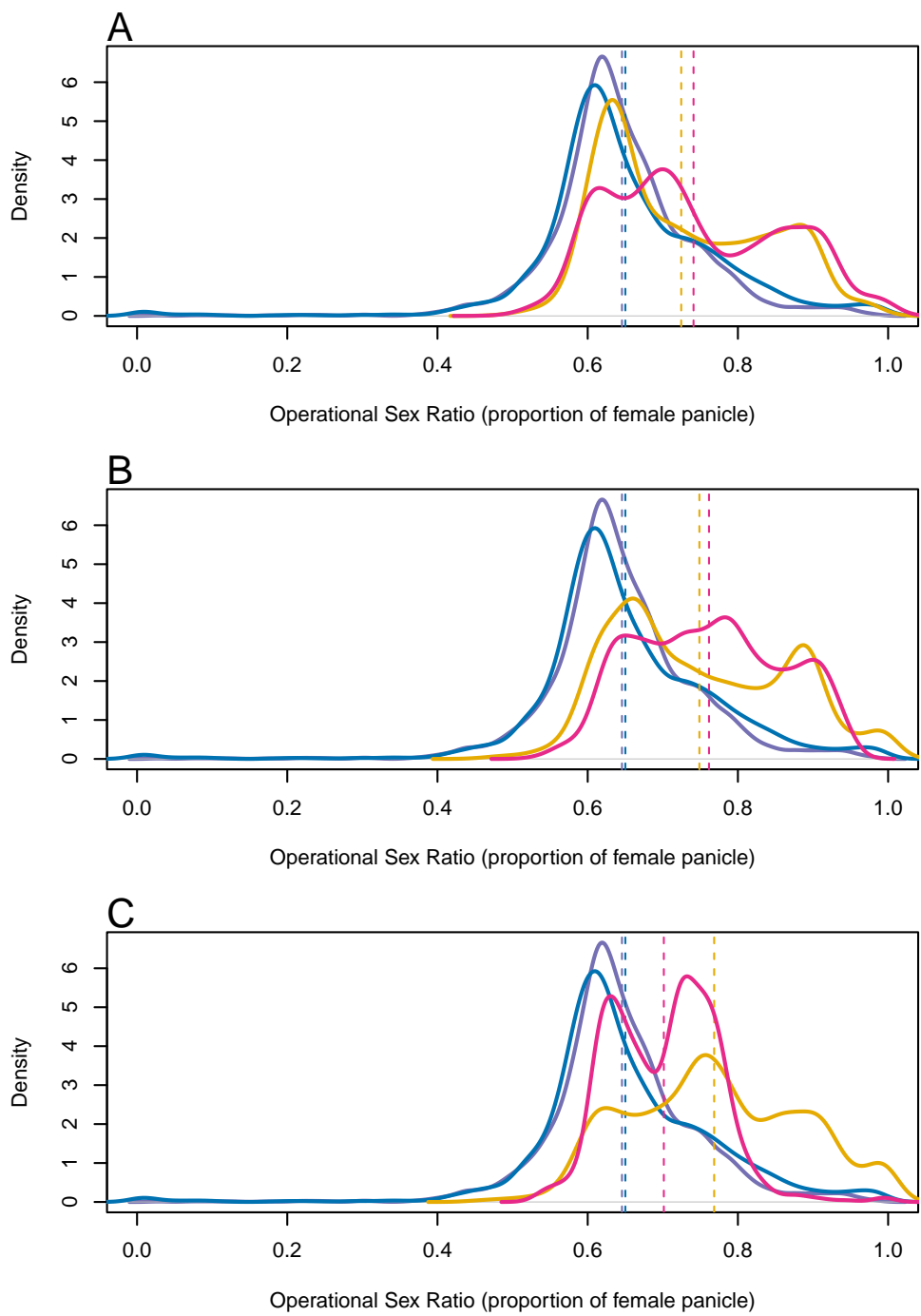


Figure S-10: Change in Operational Sex Ratio (proportion of female) over time (past, present, future). Future projections were based on A) MIROC 5, B) CES, C) ACC. The means for each model are shown as vertical dashed lines.

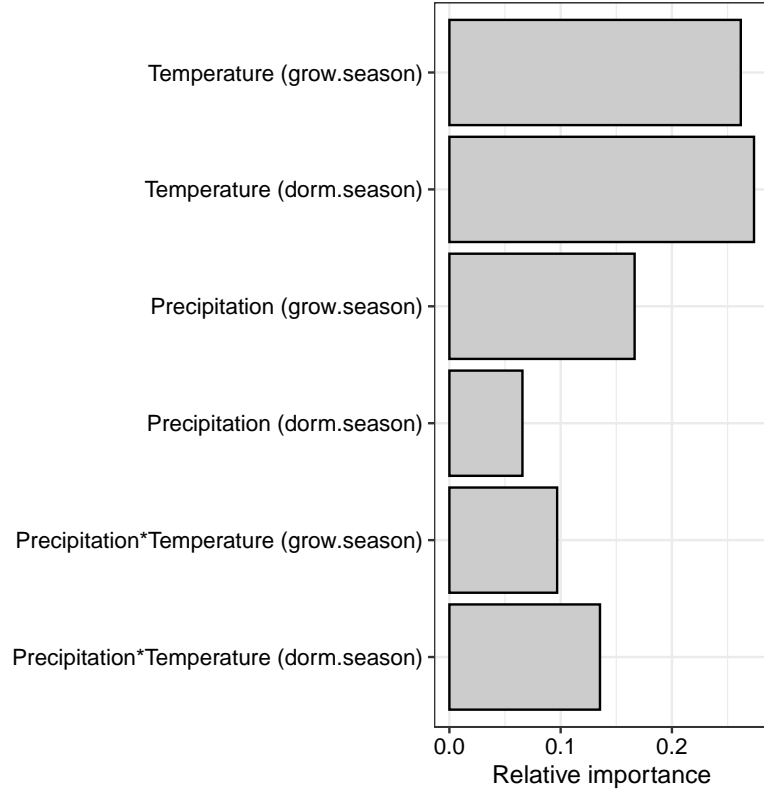


Figure S-11: Life Table Response Experiment: The bar represent the relative importance of each predictors.

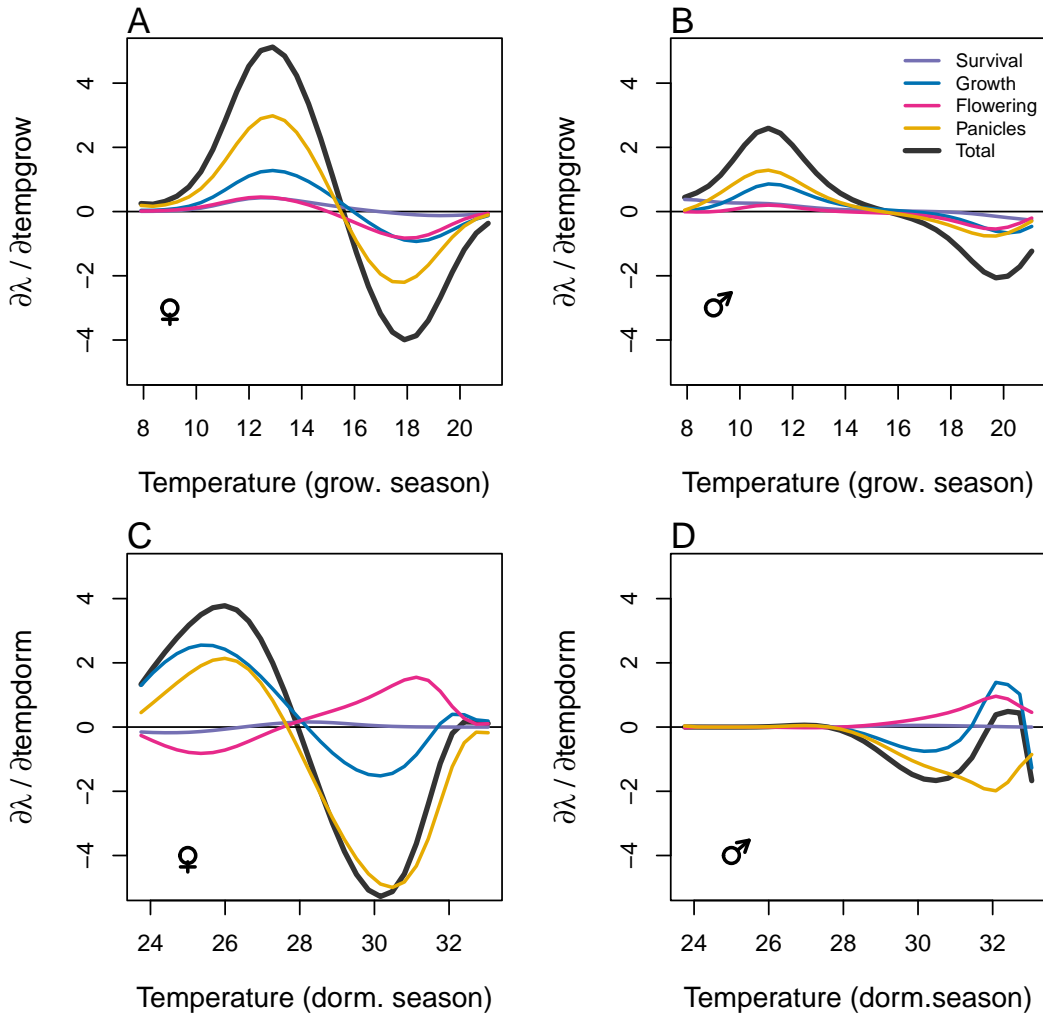


Figure S-12: Life table response experiment decomposition of the sensitivity of λ to seasonal climate into additive vital rate contributions of males and females based on posterior mean parameter estimates. (A) Temperature of growing season (contribution of female), (B) Temperature of growing season (contribution of male), (C) Temperature of dormant season (contribution of female) and (D) Temperature of dormant season (contribution of male).

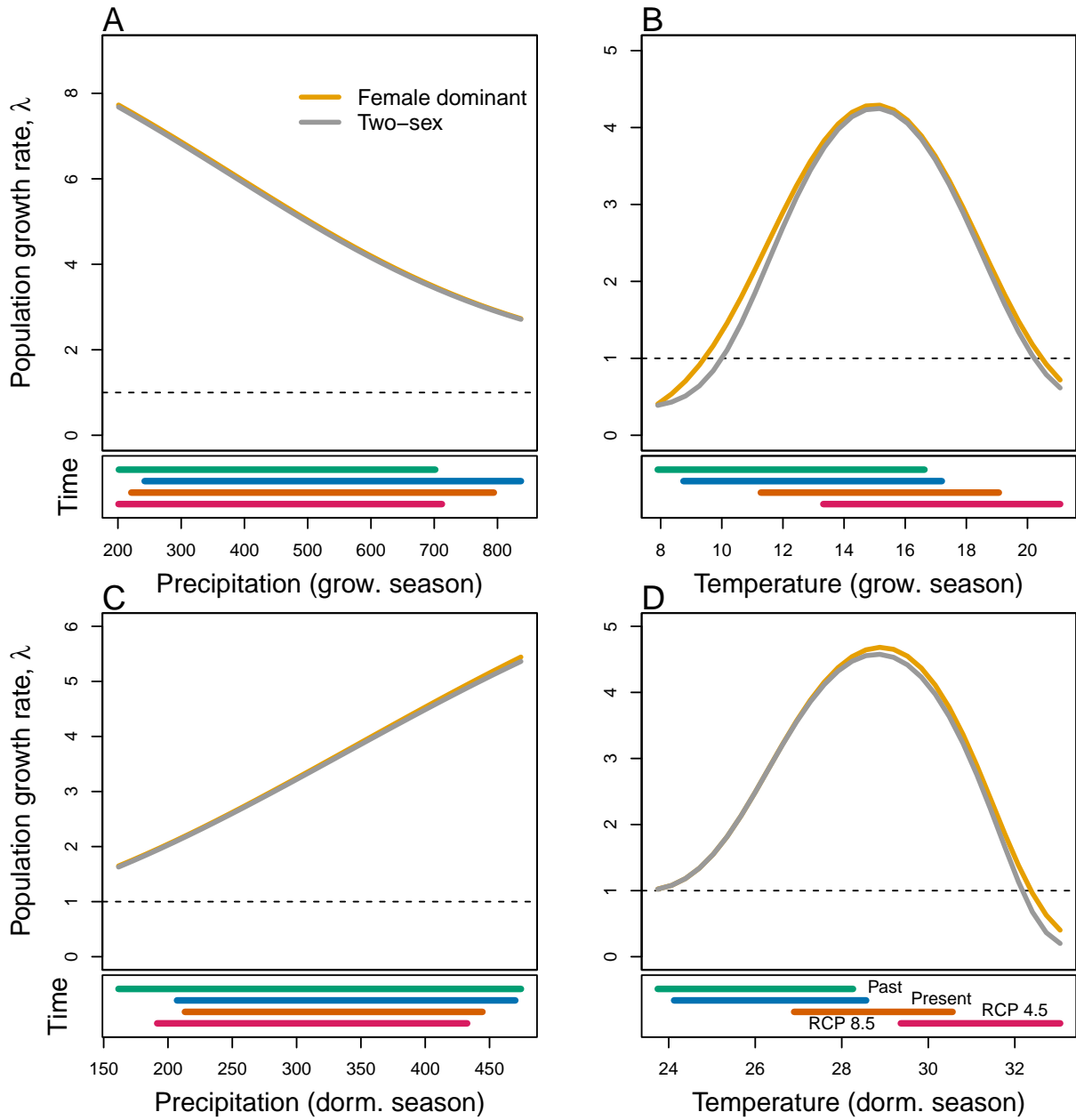


Figure S-13: Predicted population growth rate (λ) in different ranges of climate. (A) Precipitation of the growing season, (B) Temperature of the growing season, (C) Precipitation of the dormant season, (D) Temperature of the dormant season. The grey curve shows prediction by the two-sex matrix projection model that incorporates sex-specific demographic responses to climate with sex ratio dependent seed fertilization. The orange curve represents the prediction by the female dominant matrix projection model. The dashed horizontal line indicates the limit of population viability ($\lambda = 1$). Lower panels below each data panel show ranges of climate values for different time period (past climate, present and future climates). For future climate, we show a Representation Concentration Pathways (RCP) 4.5 and 8.5. Values of (λ) are derived from the mean climate variables across 4 GCMs (MIROC5, ACCESS1-3, CESM1-BGC, CMCC-CM).

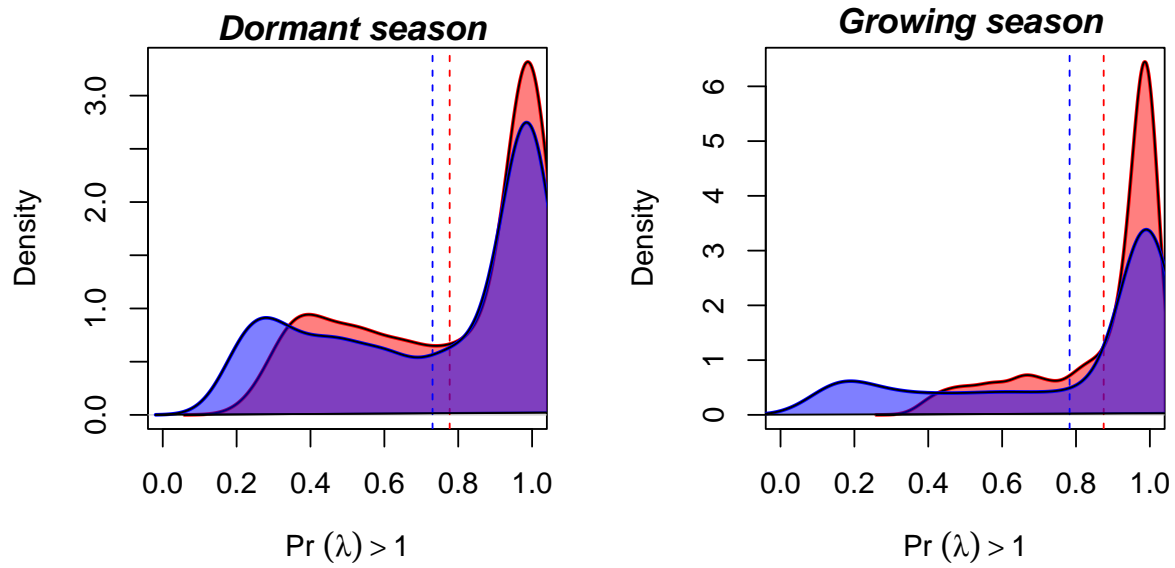


Figure S-14: Assessment of the statistical difference between the two-sex models and the female dominant model for the dormant and growing season. Plots show the density of $\Pr(\lambda) > 1$ values for female dominant (pink) and two-sex models (violet) for each season. The means for each model are shown as vertical dashed lines.

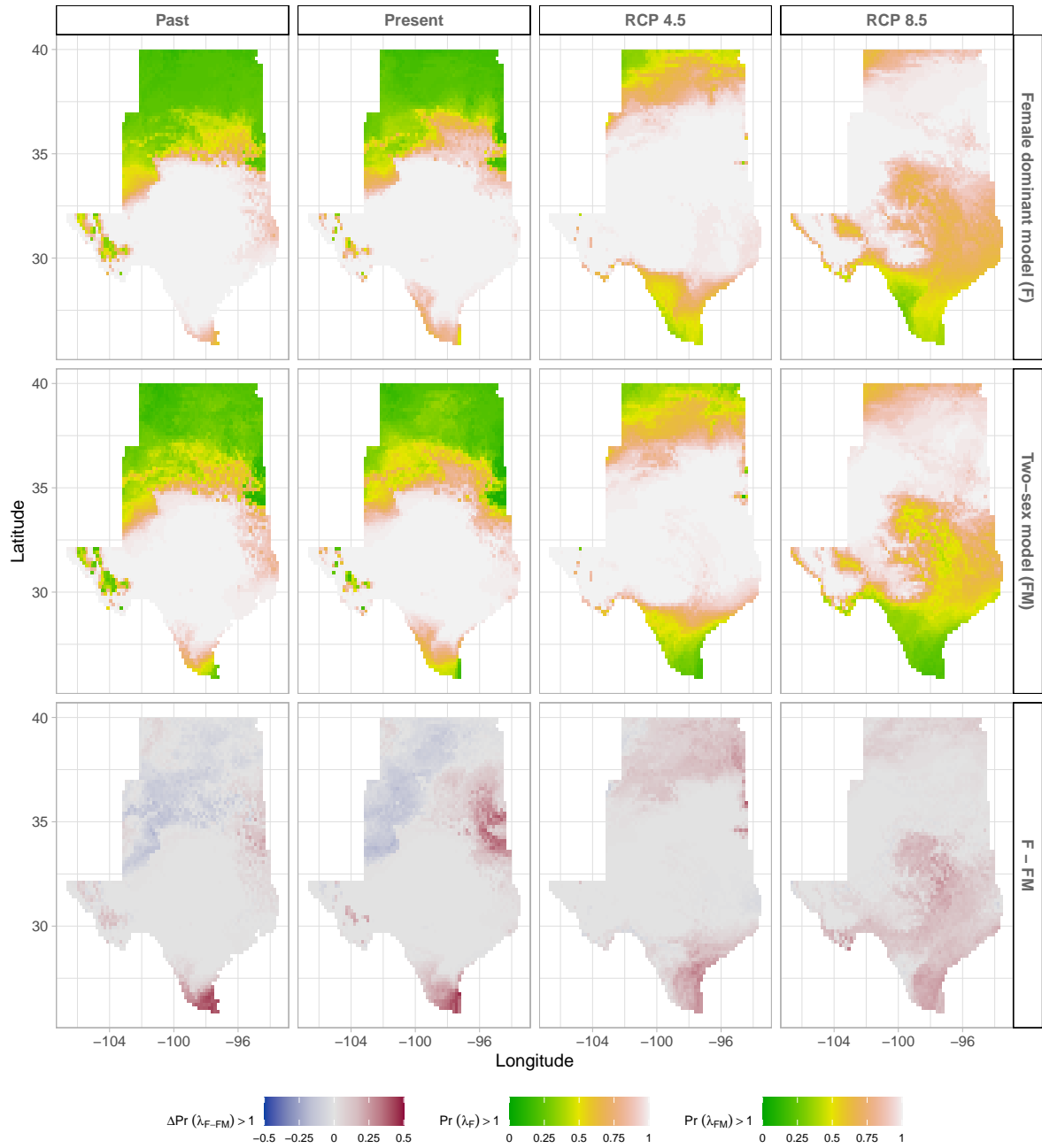


Figure S-15: Climate change favors range shift toward the North edge of the current range. (A) Past, (B) Current, (C and D) Future predicted range shift based on the predicted probabilities of self- sustaining populations, $\Pr(\lambda > 1)$, using the two-sex model that incorporates sex- specific demographic responses to climate with sex ratio dependent seed fertilization. (E) Past, (F) Current, (G and H) Future predicted range shift based on the predicted probabilities of self- sustaining populations, $\Pr(\lambda > 1)$, using the female dominant model. Future projections were based on the CESM1-BGC model. The black dots on panel B and F indicate all known presence points collected from GBIF from 1990 to 2019, which corresponds to the current condition in our prediction. The occurrences of GBIFs are distributed in with higher population fitness habitat $\Pr(\lambda > 1)$, confirming that our study approach can reasonably predict range shifts.

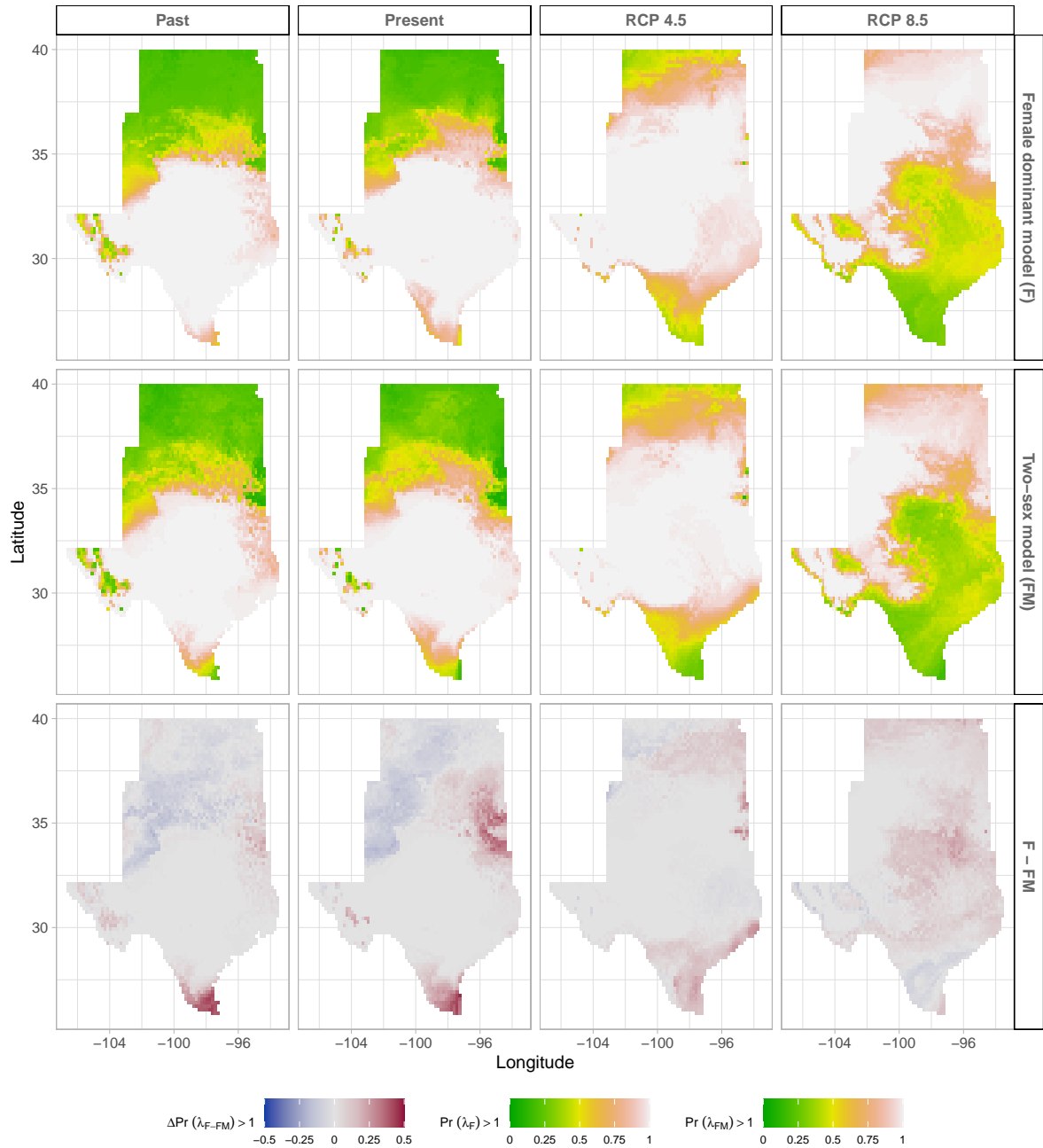


Figure S-16: Climate change favors range shift toward the North edge of the current range. (A) Past, (B) Current, (C and D) Future predicted range shift based on the predicted probabilities of self-sustaining populations, $\Pr(\lambda > 1)$, using the two-sex model that incorporates sex-specific demographic responses to climate with sex ratio dependent seed fertilization. (E) Past, (F) Current, (G and H) Future predicted range shift based on the predicted probabilities of self-sustaining populations, $\Pr(\lambda > 1)$, using the female dominant model. Future projections were based on the ACCESS model. The black dots on panel B and F indicate all known presence points collected from GBIF from 1990 to 2019, which corresponds to the current condition in our prediction. The occurrences of GBIFs are distributed in with higher population fitness habitat $\Pr(\lambda > 1)$, confirming that our study approach can reasonably predict range shifts.

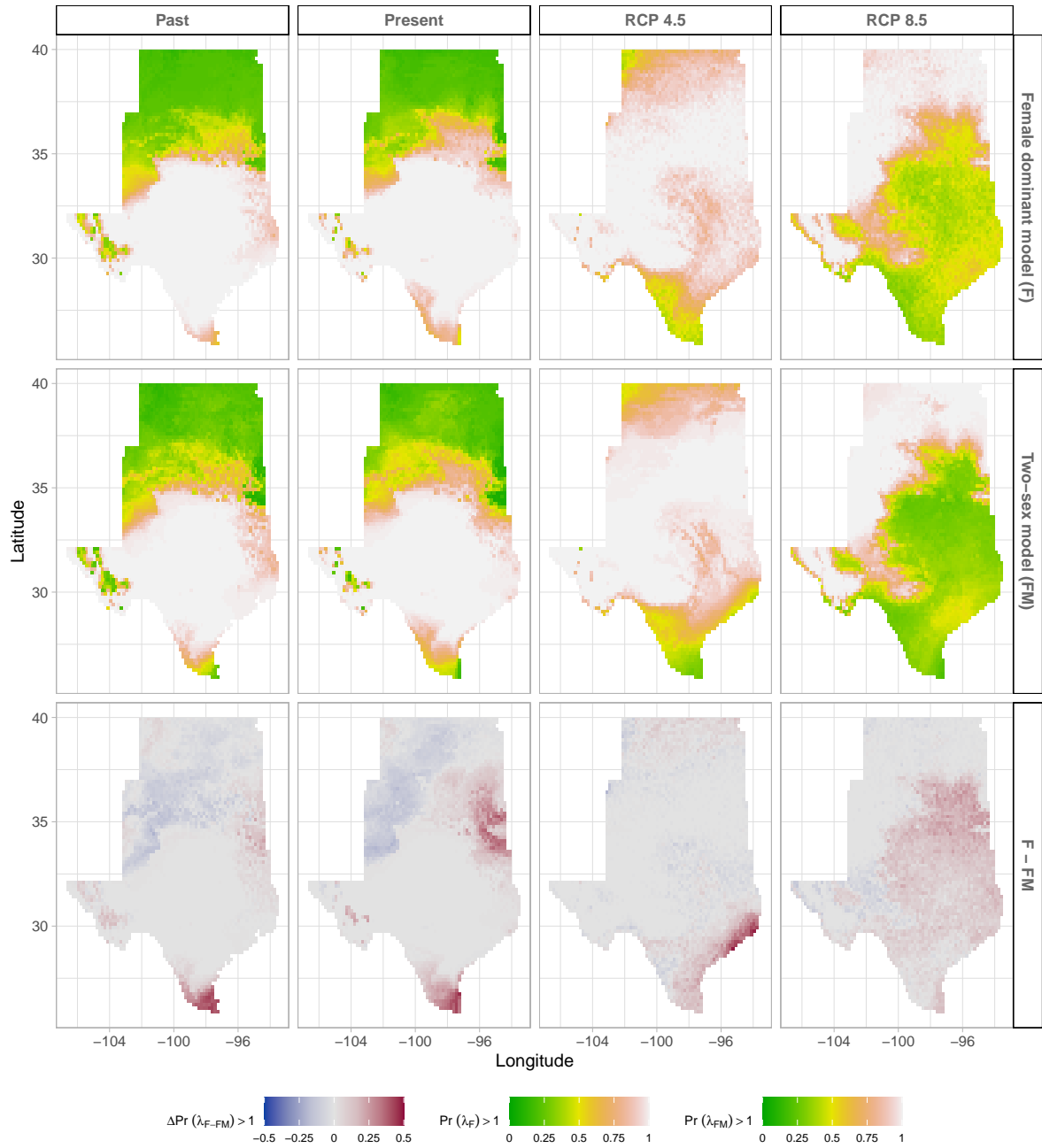


Figure S-17: Climate change favors range shift toward the North edge of the current range. (A) Past, (B) Current, (C and D) Future predicted range shift based on the predicted probabilities of self-sustaining populations, $\text{Pr}(\lambda > 1)$, using the two-sex model that incorporates sex-specific demographic responses to climate with sex ratio dependent seed fertilization. (E) Past, (F) Current, (G and H) Future predicted range shift based on the predicted probabilities of self-sustaining populations, $\text{Pr}(\lambda > 1)$, using the female dominant model. Future projections were based on the MIROC5 model. The black dots on panel B and F indicate all known presence points collected from GBIF from 1990 to 2019, which corresponds to the current condition in our prediction. The occurrences of GBIFs are distributed in with higher population fitness habitat $\text{Pr}(\lambda > 1)$, confirming that our study approach can reasonably predict range shifts.

664 **S.2 Supporting Methods**

665 **S.2.1 Sex-specific demographic responses to climatic variation across
666 common garden sites**

667 Vital rate models were fit with the same linear predictors for the expected value (μ)(Eq.S.1):

$$\begin{aligned} \mu = & \beta_0 + \beta_1 size + \beta_2 sex + \beta_3 pptgrow + \beta_4 pptdorm + \beta_5 tempgrow + \beta_6 tempdorm \\ & + \beta_7 pptgrow * sex + \beta_8 pptdorm * sex + \beta_9 tempgrow * sex + \beta_{10} tempdorm * sex \\ & + \beta_{11} size * sex + \beta_{12} pptgrow * tempgrow + \beta_{13} pptdorm * tempdorm \\ & + \beta_{14} pptgrow * tempgrow * sex + \beta_{15} pptdorm * tempdorm * sex + \beta_{16} pptgrow^2 \\ & + \beta_{17} pptdorm^2 + \beta_{18} tempgrow^2 + \beta_{19} tempdorm^2 + \beta_{20} pptgrow^2 * sex \\ & + \beta_{21} pptdorm^2 * sex + \beta_{22} tempgrow^2 * sex + \beta_{23} tempdorm^2 * sex + \phi + \rho + \nu \end{aligned} \quad (S.1)$$

669 where β_0 is the grand mean intercept, β_1 is the size dependent slopes. *size* was on a natural
670 logarithm scale. $\beta_2 \dots \beta_{13}$ represent the climate dependent slopes. $\beta_{14} \dots \beta_{23}$ represent the
671 sex-climate interaction slopes. *pptgrow* is the precipitation of the growing season, *tempgrow*
672 is the temperature of the growing season, *pptdorm* is the precipitation of the dormant season,
673 *tempdorm* is the temperature of the dormant season.

674 **S.2.2 Sex ratio responses to climatic variation across common garden sites**

675 To understand the impact of climatic variation across common garden sites on sex ratio, OSR
676 and SR models using the same linear predictors for the expected value (ν)(Eq.S.2):

$$\begin{aligned} \nu = & \omega_0 + \omega_1 pptgrow + \omega_2 pptdorm + \omega_3 tempgrow + \omega_4 tempdorm + \\ & \omega_5 pptgrow^2 + \omega_6 pptdorm^2 + \omega_7 tempgrow^2 + \omega_8 tempdorm^2 \end{aligned} \quad (S.2)$$

678 where OSR is the proportion of panicles that were female or proportion of female individuals
679 in the experimental populations, c is the climate. ω_0 is the intercept, $\omega_1, \dots, \omega_8$ are the climate
680 dependent slopes.

681 **S.2.3 Sex ratio experiment**

682 To estimate the probability of seed viability, the germination rate and the effect of sex-ratio
683 variation on female reproductive success, we conducted a sex-ratio experiment at one site
684 near the center of the range to estimate the effect of sex-ratio variation on female reproductive

685 success. The details of the experiment are provided in Compagnoni et al. (2017) and Miller
686 and Compagnoni (2022b). Here we provide a summary of the experiment. We established
687 124 experimental populations in plots measuring 0.4 x 0.4m and separated by at least 15m
688 from each other. We varied population density (1-48 plants/plot) and sex ratio (0%-100%
689 female) across the experimental populations, and we replicated 34 combinations of density
690 and sex ratio. We collected panicles from a subset of females in each plot and recorded the
691 number of seeds in each panicle. We assessed reproductive success (seeds fertilized) using
692 greenhouse-based germination and trazolium-based seed viability assays. Seed viability was
693 modeled with a binomial distribution where the probability of viability (v) was given by:

694
$$v = v_0 * (1 - OSR^\alpha) \quad (\text{S.3})$$

695 where OSR is the proportion of panicles that were female in the experimental populations.
696 α is the parameter that control for how viability declines with increasing female bias. Further,
697 germination rate was modeled using a binomial distribution to model the germination
698 data from greenhouse trials. Given that germination was conditional on seed viability, the
699 probability of success was given by the product $v * g$, where v is a function of OSR (Eq. S.3)
700 and g is assumed to be constant.